The GRACE event calendar

Bramha Dutt Vishwakarma

Supervisors: Prof. Dr.-Ing. Nico Sneeuw , Balaji Devaraju &
Dr. Kamal Jain

Institute of geodesy, University of Stuttgart

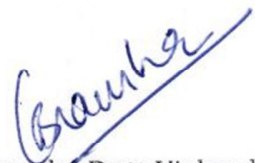Geomatics engineering group, Indian Institute of Technology

11/06/2012

Candidate's Declaration

This is to certify that this thesis work titled "GRACE event calendar" has been carried out in the Institute of geodesy, University of Stuttgart, Germany and Geomatics engineering group, Department of civil engineering, Indian Institute of Technology, Roorkee, India under the supervision of Prof. Dr.-ing Nico Sneeuw, Balaji Devaraju and Dr. Kamal Jain. This work was carried out under DAAD master-sandwich exchange program.

Place: Stuttgart

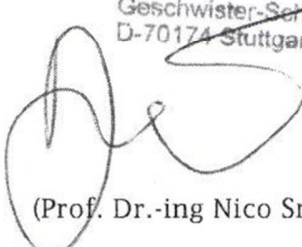Date: 11|6|12

(Bramha Dutt Vishwakarma)

Forwarded

(Dr. Kamal Jain)

Place: Roorkee

Date: 11|6|12

Institute of Geodesy
Universität Stuttgart
Geschwister-Scholl-Str. 24D
D-70174 Stuttgart, Germany

(Prof. Dr.-ing Nico Sneeuw)

Place: Stuttgart

Date: 11.06.2012

Acknowledgements

Abstract

GRACE mission is a joint venture of NASA and GFZ. This mission was launched to provide with unprecedented accuracy, estimates of the global high resolution models of the Earth's gravity field. The study of time-variability of Earth's gravity field is very helpful in climate sciences and earth's sciences studies. People have done a lot of work to demonstrate the effect of many natural phenomenon on gravity. Gravity estimates from GRACE are used for estimating mass redistribution at continental scale. So, we can observe hydrology, seismology and glaciology potential areas where GRACE can be useful.

This research work focuses on identifying the hydrological events such as floods and drought, seismic events such as earthquakes and volcanic activity and also the glacier melting in the GRACE time-series. The work includes the development of strategy for the analysis of these events keeping in mind their behaviour and GRACE limitations of spatial resolution and sensitivity. Further in this work we would produce a event calendar for such events stating whether gravity changes caused by such events are visible to GRACE.

Calendars are generated for hydrological events, floods and droughts separately and also for earthquake events. For rest of the phenomenon we have not generated calendars since these events are very few in numbers. This work is a qualitative analysis, so we could observe whether GRACE signal is able to observe these events or not. Hydrological events are observed by searching outliers in the grace observed time-series. The large floods such as 2009 Amazon floods can be seen when we take whole catchment, but the small floods affecting smaller region such as Sao Paulo flood is not visible in catchment time-series, so we have to go for selected area time-series generation. The factors such as time period for floods and droughts are very important factors when we want to observe them by GRACE. Earthquakes visibility depends on range rate amplitude, and also the quality of ΔC_{20}, we have discussed these aspects while analysing earthquakes occurred in last decade from GRACE. We have given the possible explanation for the events not visible, and those visible have helped in the development of a methodology for analysis of a particular event. The volcanic activity in Caldera and Bolivia are pushing earth upward so we can expect some signal, but the spatial extent of these areas is small with caldera area greater than that of Bolivia, only caldera showed a trend. We also did trend analysis for 2 Asian glaciers and a part of Greenland for observing the melting of these ice masses. The work finally produces a series of events which we were able to observe by GRACE and we also get the methodology suitable for analysis of an event.

Contents

List of Figures

3

4

List of Tables

Chapter 1

Introduction

For the past few decades man has been regularly trying to model various natural phenomenon, to demonstrate their affect on various physical properties of earth and its environment and vice-versa. Amongst these the most influential factor, through which these global events are reflected is gravity. Gravity monitoring thus became an inevitable requirement to study Earth and its behaviour. People have worked in this direction starting from land gravimetry since 1817 with Katers pendulum. With the profound development in satellite and rocket sciences mankind thought of gravity monitoring by satellites. For the few decades, the tracking of artificial satellites in Earth's orbit has been principle means of determining the Earth's gravity field. Since, the orbital motion depend on the gravitational field of earth, hence by knowing orbit we can track gravity. But, the need of dedicated satellite gravity missions was felt strongly when we needed to map gravity at global scale and at regular interval of time for climate sciences and earth sciences. CHAMP was first dedicated satellite gravity mission but the spatial resolution was around 800 km for EIGEN-1S Earth gravity field model. This model involved spherical harmonic coefficient terms up to degree and order 35. Also CHAMP could not study the time-variability of earth's gravity field. With time now we have EIGEN-CHAMP03S Earth gravity model which provides gravity field at an resolution of 400 km but, at that time necessity for a mission providing high resolution gravity model along with time-variability of earth's gravity was felt. Second dedicated gravity mission GRACE was thus proposed. GRACE was launched on 17 march 2002 as a joint venture of NASA and GFZ.

GRACE is a valuable mission giving Earth's gravity field at monthly intervals. The mission gravity recovery and climate experiment is mapping the global gravity field with a spatial

resolution of 400 km to 4,000 km every thirty days (Schmidt [2008]). The changes in local gravity is due to redistribution of mass, which can be due to many nature driven activities. We can study GRACE observed mass changes with the motivation to study the hydrology, glaciology, and seismology of an area. There lies a lot of potential in this mission which needs to be illuminated. The work discussed in this master thesis is qualitative, we would not look for quantitative validation for our findings in this thesis work. The events related to above mention fields impart a change in local gravity so, we would ask whether these events are visible to GRACE? How the change introduced by these events are reflected in GRACE observed time-series and how much change is enough to be detected, their spatial extent is whether good enough for GRACE? We would not quantify the answers to these questions rather we would like to quote which event, at what intensity and spatial extent was visible to GRACE. The possible explanation to invisibility of few events would also be illuminated. This chapter would discuss the motivation behind work and its importance.

1.1 Motivation behind work

The work done till now in hydrology, was basin water cycle study, modelling of basin, terrestrial water storage changes and so on. There was a work by Florian Seitz [2008] which focused on detecting European heat waves with GRACE. This motivated us to look into other aspects of hydrology such as floods and droughts, whose occurrence produces a large mass redistribution and destruction to mankind and property. The events related to hydrology are said to have high probability of occurrence after a certain time, and in recent decades their frequency has been observed to increase as told by an article "dried up, drowned down". This work is using GRACE data set for the period of 8 years. We would look for these events in the GRACE observed time-variability of Earth's gravity.

Similarly, earthquakes produce a large and sudden mass redistribution. Few of them having high energy processes involved must be visible in the GRACE data set. We also discussed the limit of magnitude of Earthquake, above which they stand a fair chance of being seen by GRACE. Volcanic activities also produce mass redistribution, but for them to be visible to GRACE the activity should be of high magnitude and spatial extent. We figured out such two volcanoes and analysed them to see the rise in one of them.

Glaciers are receding at fast rates concerning mankind about rising sea level. Studying

glaciers has been an important topic since the last decade. The continuous observations of glaciers whether by air-borne RADAR data, or in-situ observations is very difficult. Satellite observations provide continuous data and they have been verified by other data, thus GRACE provides that extra edge. We would do trend analysis for few glaciers.

1.2 Outline of thesis work

This thesis starts with the description of GRACE mission and its objectives in chapter 2. The organisations involved in providing us the data and we would also describe the data set used in this chapter. Then in chapter 3 the basic mathematics behind expressing the gravity potential variations in terms of spherical harmonic coefficients, the mathematical relations involved and necessary for understanding are discussed. Then later in this chapter we would look at the spectral domain behaviour of the data and the post processing done in order to get the desired format of residual coefficients. The modification of data set to fulfil our requirements and to take care of errors involved including trade-off between two factors are brought into light. The later part of this chapter would tell about global gravity map generation and expressing the potential variations in different terms.

Chapters 4, 5 and 6 involves identifying the hydrology, seismology and glaciology related events recorded by GRACE. Then in each section we would identify the factors important for visualising these events and how we can enhance the visualisation. Then we would discuss few events that occurred during the life time of GRACE, their visibility and non-visibility in the data set are explained with reasons having high probability. Then we would come up with event calendar to sum up each event.

In chapter 7 we would come up with conclusions drawn from the thesis work and the possible future scope of this work.

Chapter 2

GRACE mission and its objective

2.1 GRACE mission

Since last few decades human beings have gained expertise in space science. Observation of our planet from Space has several benefits such as global coverage and better temporal resolution. Other than communication and broadcasting, satellites are very useful for studying our planet. Gravity change is simply responsible for many natural phenomena. It is responsible not only for occurrence of many natural events but it is also affected by various natural events across the globe. Monitoring gravity became very essential for carrying out a close surveillance on how planet is behaving over time. For past few decades tracking of artificial satellites in the Earth orbit has been the principle means of determining the Earth's gravity field. Since the motion of satellites is largely dependent on gravity field thus we can invert the orbit solutions based on satellite tracking observation to get the gravity field (John Wahr [1998]). The missions such as LAGEOS and CHAMP were there to observe gravity changes, but due to high altitude of Laser Geodynamics Satellites (LAGEOS) it provided gravity information at longer wavelength thus ending up with poor spatial resolution. CHAMP being the first dedicated satellite gravimetry mission was highly useful but due to its poor accuracy and resolution we needed a new dedicated satellite gravimetry mission. This mission was named GRACE (John Wahr [1998]).

Gravity Recovery And Climate Experiment (GRACE) is a joint mission of National Aeronautics and Space Administration (NASA) and the Deutsches Zentrum fr Luft-und Raumfahrt (DLR). It was launched on March 17 2002 with an objective to provide with unprecedented accuracy, estimates of the global high resolution models of the Earths gravity field for a period
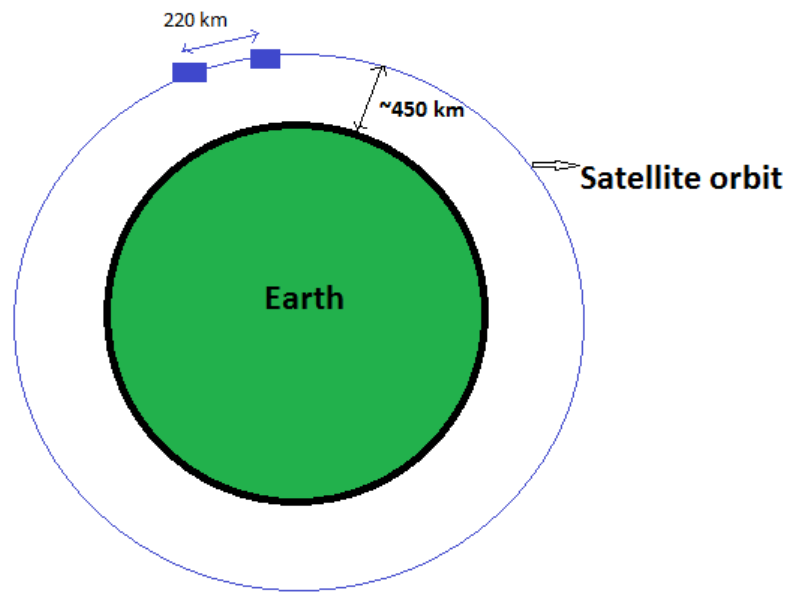
Figure 2.1: GRACE satellite visualisation

of up to five years, now it has successfully completed its ten years. The mission was proposed in 1996 jointly by the University of Texas at Austin, Center for Space Research (UTCSR), the GeoForschungsZentrum Potsdam (GFZ), the Jet Propulsion Laboratories (JPL), Space Systems/Loral (SSL), the Deutsches Zentrum fr Luft-und Raumfahrt (DLR), and Astrium GmbH. (cite: utcsr website)

GRACE satellite consists of two satellites orbiting Earth at an altitude of 480-500 km one following other, maintaining an inter-satellite distance of 220 km. The basic idea is to trace the spatio-temporal gravity field from precise inter-satellite range measurement and range rate observation (Schmidt [2008]).These two satellites are in a near polar orbit with inclination of 89.5 degrees. They maintain a two-way microwave-ranging link between them, a K/ka-band microwave link for low-low Satellite-to-Satellite tracking (ll-SST) measurements. Accurate distance measurements are made by comparing frequency shifts of the link. As a cross-check, the satellites measure their own movements using accelerometers. All of this information is then downloaded to ground stations. Now the question arises why there would be distance change between the two satellites? This can be explained as follows: the orbital motion is largely defined by the gravity field in which the satellite is moving. If we have a varying

gravity field the satellite would move in an orbit fluctuating from a regular elliptical orbit. We have two satellites linked to each other, at a certain distance from each other in space. So, if one of them experiences a different gravity field than the other then there would be variation in its position, thus variation in the distance with respect to the other satellite. If over time there is a mass redistribution we would also observe range changing with time for same location. If we know the range rate we can derive the local gravity change, because the range rate is directly proportional to the integral of gravity difference experienced by the two satellites (Schmidt [2008]).

The absolute positioning of the two spacecraft and the inter-satellite observation, which is required to be in an Earth fixed frame is obtained with GPS receivers on-board each GRACE satellite. For determination of absolute and relative orientation of the observation in space each satellite carries two star camera assemblies. To account for non-conservative contributions they have capacitive accelerometer. Additionally a laser retro reflector is placed at nadir looking panel of each satellite. Based on precise laser ranging data from the ground station network of the International Laser Ranging Services (ILRS), verification and calibration of GPS receivers and the K-band instrument is done (Schmidt [2008]).

The observations of K-band measurements are received at ground stations where they are processed by the teams of Science Data System (SDS) to produce set of spherical harmonic coefficients for each month. Thus the data product is time series consisting of monthly sets of fully normalized spherical harmonic coefficients of the global gravity potential of the Earth. GRACE satellites revolve round the Earth 15 times a day. For better global coverage and good spatial resolution we need to look at aggregated monthly data set, since the more the number of revolutions in non-repeat orbits better would be spatial resolution. Thus there is a compromise between spatial and temporal resolution. For monthly fields we obtain a spatial resolution of approximately 400 km.

2.2 Data description

Initial GRACE gravity model GGM01S (UTCSR) and EIGEN_/GRACE01S (GFZ) were determined using the GRACE measurements. The GGM01S model was derived using first 111 days data by using a conventional dynamic least-square adjustment. The difference between the GRACE observations of range-rate and the range-rate predicted by the nominal orbit were ingested

into a large least-square problem solving for updates to the spherical harmonic coefficients of the geopotential. This GGM01S model was developed by GRACE observations only and then it was compared to a pre GRACE model, EGM96 (B. D. Tapley [2004]). EGM96 was developed by combining data from over a thirty-year period of tracking near Earth satellites, satellite altimetry data over the oceans and an extensive set of land-based measurements. The error estimates in the model were obtained by an approximate caliberation of the formal error covariance based on internal sub-set solution comparisons. On comparison with EGM96, the 111 days of data had an improved accuracy by over an order of magnitude for long and mid wavelength components of the Earth gravity field model. The calibrated errors indicated a global RMS error of 2 cm to degree and order 70, uniformly over land and ocean. These models are significantly improved in quality over time through several complete iterations and reprocessing of the steadily increasing GRACE data set. We have different releases by SDS team, latest is the release number four (labeled RL04). It covers almost the whole mission period from 2002 to 2011, and it is based on the latest processing standards and strategies. This data set is labeled GFZ-RL04 in the SDS terminology respectively EIGEN-GRACE04S.

2.2.1 Data used

Release 04 level 02 data from GFZ is used in this thesis work. The Release 04 level 02 data used is from GFZ consisting of monthly spherical harmonic coefficients up to order and degree 120. The GRACE data releases include estimates of calibrated errors in the stokes coefficients: diagonal elements of the covariance matrix, rescaled by the project to match certain characteristics of the fields. These error estimates include measurement and processing errors (John Wahr [2006]). Data used is from August 2002 till May 2011 with data from certain months completely missing and few having repeat orbit problem for which we have regularized solution. We stick to the normal GFZ gravity solutions instead of its regularized solution for this thesis work.

While a satellite is in repeat orbit mode the orbits are not evenly distributed over the globe. This condition affects badly the resolution and quality of gravity field estimates. To determine whether there are repeat orbits in any month we can apply a simple check. If the ratio between numbers of revolutions (β) that the satellite fulfils in a number of days (α) is an integer ratio then it is not a repeat orbit. GRACE is more sensitive to along track measurements and we want a good distribution of orbits over the globe for better spectral resolution and less

north south stripes. Thus due to repeat orbit the north-south stripes are more prominent for that month data. GFZ also releases the regularized solution for such repeat orbit months. The numerical singularities are due to the measurement concentrated along the repeated ground tracks and we need regular grid spread all over the globe. They generate the data for more dense orbits by methods of regularization (Bentel [2009]).

2.3 Objectives and science application of the mission

The primary science objective of the GRACE mission is to provide with unprecedented accuracy, global and high-resolution estimates of the constant and time-variable part of the Earth's gravity field. Secondary objective is the measurement of several hundred globally distributed profiles per day of the excess delay or bending angle of GPS measurements caused by the atmosphere and ionosphere, which can be converted to total electron content and/or refractivity, respectively. Typical GRACE Science Applications are the improved knowledge of the mean geoid, which lead - in conjunction with altimetry and *in-situ* data - to significant advances in oceanographic, geodetic or solid Earth science studies such as

- oceanic heat flux,

- long term sea level change,

- upper oceanic heat content,

- absolute surface geotropic ocean currents or

- Precise positioning, orbit determination and leveling.

Estimates of time variable components of the gravity field help for a better understanding of time variable processes in oceanography, hydrology, glaciology or solid Earth sciences like

- deep ocean current changes,

- large-scale evapotranspiration,

- soil moisture changes,

- mass balance of ice sheets and glaciers,

- changes in the storage of water and snow of the continents,

- mantle and lithospheric density variations,

- glacial isostatic adjustment,

- Post seismic and pre seismic effects of seismic activities such as earthquakes.

Chapter 3

Converting gravity potential to mass and generation of global gravity maps

Gravity potential variation at a location is mainly due to mass change at that place. We can represent potential variations over a sphere by spherical harmonics. When we talk about the spherical harmonic function, the product of Legendre functions and Fourier series. We are interested in representing the potential. We are working in spectral domain when we say we work on spherical harmonic coefficients, but we are interested in studying the mass redistribution on earth surface, which is a spatial domain entity. Thus we need to travel from frequency domain to spatial domain. In this chapter we will introduce the mathematical base necessary to understand the GRACE data and its physical representation. The mathematical background starts with potential theory. Potential variations can be represented in terms of spherical harmonic coefficients. If we have spherical harmonic coefficients we can get back the potential variations, and which further can be converted to mass. The next section would throw some light on potential theory and on the role of spherical harmonic coefficients in estimating the Earth's potential field.

3.1 Potential theory and mathematical foundation

Newton published his work on gravitation in 1687 named *philosophiae naturalis principia mathematica*. He made fundamental observations and gave the relation for gravitational force.

$$F = G\frac{m_1 m_2}{r^2} \tag{3.1}$$
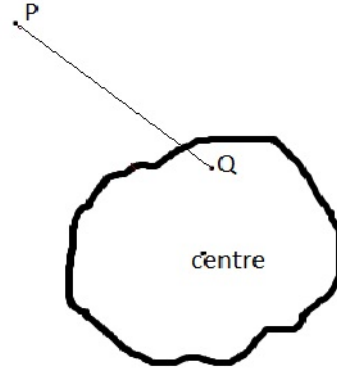
Figure 3.1: Body experiencing density change at Q and potential change observed at P

The gravitational attraction is the force experienced by the two bodies so they would have some acceleration which is calculated further by replacing the force as product of mass and acceleration felt by one of the mass. Thus gravitational acceleration is:

$$g = G\frac{m_2}{r_{12}^2} \tag{3.2}$$

its unit is m/s² also called Gal; 1 Gal= 10^{-2} m/s².

Gravitational force is a conservative field and gravitational attraction is not acceleration, it is dynamical quantity: attraction per unit mass. When we are able to define a force due to some conservative vector field then the vector is generated by a scalar potential field. When we are willing to move from one equipotential surface to other we experience work done either by us or by field. The condition of conservative field is stated as: the work done in moving from one point to other is same whichever path is followed. The movement from one potential to other involves energy transformation and for movement between same potential no energy is required. The satellite motion largely depends on this potential. We should start with potential.

Figure 3.1 shows the observation point P and the point where there is a density change denoted by Q. Newton's law for potential change observed at P due to density change at Q yields the relation:

$$\delta V_{\mathrm{P}} = G \int \int \int \left(\frac{\Delta \rho_{\mathrm{Q}}}{l_{\mathrm{PQ}}} d\Sigma_{\mathrm{Q}} \right) \tag{3.3}$$

20

wherein G is the universal gravitation constant, $\Delta\rho_Q$ is the change in density at Q, l_{PQ} is the distance between P and Q and $d\Sigma_Q$ represents elementary volume at Q.

We can express the reciprocal distance into Legendre polynomial. This potential expression is derived from the Laplace equation and the boundary conditions. It is valid for the object on or above the surface of Earth. When we expand the reciprocal distance into Legendre polynomials we get

$$\frac{1}{l_{PQ}} = \frac{1}{r_P} \sum_{n=0}^{\infty} \left(\frac{r_Q}{r_P}\right)^n P_n(\cos\psi_{PQ}) \tag{3.4}$$

Where in $P_n(\cos\psi_{PQ})$ is Legendre function, n denotes the degree and r_P and r_Q are distance of point P and Q from centre. Further according to the addition theorem of Legendre functions we can expand the Legendre polynomial, The addition theorem is given by:

$$P_n(\cos\psi_P) = \frac{1}{2n+1} \sum_{m=0}^{n} [\cos m\lambda_P \cos m\lambda_Q + \sin m\lambda_P \sin m\lambda_Q] \bar{P}_{nm}(\cos\theta_P) \bar{P}_{nm}(\cos\theta_Q) \tag{3.5}$$

where $\bar{P}_{nm}(\cos\theta)$ denote the fully normalized associate Legendre-polynomials. λ and θ are longitude and co-latitude respectively. Divide and multiply by $a^{(n+1)}$, where a is radius of the Earth. After applying addition theorem and replacing $P_n(\cos\psi_{PQ})$ we get.

$$\delta V_P = \frac{GM}{a} \sum_{n=0}^{\infty} \left(\frac{a}{r_P}\right)^{(n+1)} \sum_{m=0}^{n} \frac{1}{M(2n+1)} \int_{\Sigma} \left(\frac{r_Q}{a}\right)^n \delta\rho_Q \bar{P}_{nm}(\cos\theta_Q) \cos m\lambda_Q d\Sigma_Q \cos m\lambda_P \bar{P}_{nm}(\cos\theta_P)$$

$$+ \frac{1}{M(2n+1)} \int_{\Sigma} \left(\frac{r_Q}{a}\right)^n \delta\rho_Q \bar{P}_{nm}(\cos\theta_Q) \cos m\lambda_Q d\Sigma_Q \sin m\lambda_P \bar{P}_{nm}(\cos\theta_P) \tag{3.6}$$

$$\delta V_P = \frac{GM}{a} \sum_{n=0}^{\infty} (\frac{a}{r_P})^{(n+1)} \sum_{m=0}^{n} \Delta C_{nm} \cos m\lambda_P \bar{P}_{nm}(\cos\theta_P) + \Delta S_{nm} \sin m\lambda_P \bar{P}_{nm}(\cos\theta_P) \tag{3.7}$$

where

$$\Delta C_{nm} = \frac{1}{M(2n+1)} \int_{\Sigma} \left(\frac{r_Q}{a}\right)^n \delta\rho_Q \bar{P}_{nm}(\cos\theta_Q) \cos m\lambda_Q d\Sigma_Q \tag{3.8}$$

$$\Delta S_{nm} = \frac{1}{M(2n+1)} \int_{\Sigma} \left(\frac{r_Q}{a}\right)^n \delta\rho_Q \bar{P}_{nm}(\cos\theta_Q) \cos m\lambda_Q d\Sigma_Q \tag{3.9}$$

The M, mass of the Earth can be written as product of volume and average density which is:

$$M = \frac{4\pi a_3 \bar{\rho}}{3} \tag{3.10}$$

21

for constant r_Q we have to integrate the surface only so the volume integral would be now surface integral. Expressing the spherical harmonic coefficients in terms of density variation:

$$
\begin{pmatrix} \Delta C_{nm} \\ \Delta S_{nm} \end{pmatrix} = \frac{3}{4\pi\bar{\rho}a} \frac{1}{2n+1} \int \int_s \left[\int \delta\rho(\theta_Q, \lambda_Q, r_Q) \left(\frac{r_Q}{a} \right)^{(n+2)} dr_Q \right]
$$

$$
\bar{P}_{nm}(\cos\theta_Q) \begin{pmatrix} \cos m\lambda_Q \\ \sin m\lambda_Q \end{pmatrix} ds_Q \quad (3.11)
$$

The time dependent (dimensionless) spherical harmonic coefficients $\Delta C_{nm}(t)$, $\Delta S_{nm}(t)$ represent the mass distribution generating the field at an instant moments of time. ds_Q denotes surface element. This spherical harmonic solution originated from solving the Laplace equation in spherical coordinate system. Few important properties of spherical harmonics are discussed in Appendix [Nico Sneeuw, lecture notes Physical geodesy]:

These spherical harmonic coefficients are very useful as they reveal a lot about earth surface, C_{00} represents the total mass, the coefficients of degree 1 represent the coordinates of the earths centre of mass in our chosen coordinate system, if the coordinates coincide with the centre of mass then; $C_{10} = C_{11} = S_{11} = 0$. The coefficient of degree 2 and order 0, C_{20} is proportional to the flattening of earth, i.e. the permanent deformation caused by earth rotation leading to an ellipsoidal shape of the earth instead that of a sphere.

3.2 Spectral domain analysis and modification of data

When we get the data we are always interested in the frequency domain analysis of data since it provides a view point which spatial data cannot, for example the processing is easier as the convolution in spatial domain is multiplication in spectral domain and data size is smaller. The coefficients in a monthly data set are correlated and noisy. The extent of correlation and noise is very important to understand to decide which coefficients carries more signal and less noise. We used degree variance curve to study signal and noise power behaviour in GRACE data.

The GRACE data degree variance curve helps us to visualize the variation in power of noise and signal with degree of the coefficients. The degree variance of a signal in terms of spherical harmonic coefficients is given by:
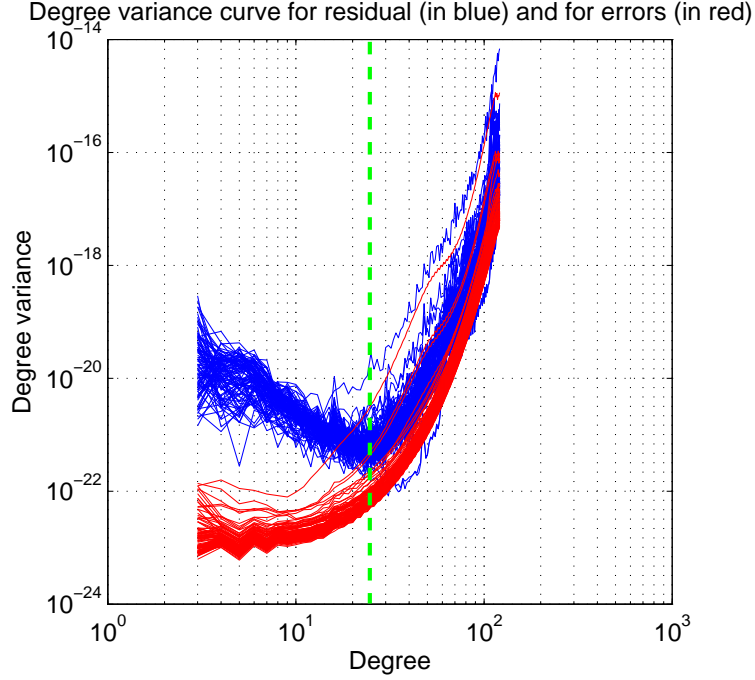
Figure 3.2: Degree variance curve for GRACE signal and error

$$\sigma_n^2 = \sum_{m=0}^{n} (C_{nm}^2 + S_{nm}^2) \tag{3.12}$$

$$\epsilon_n^2 = \sum_{m=0}^{n} (\epsilon_{C_{nm}}^2 + \epsilon_{S_{nm}}^2) \tag{3.13}$$

σ_n^2 and ϵ_n^2 are signal degree variance/power and error degree variance/power of a certain degree n of spherical harmonic signal respectively.

The figure shows that the error power is initially low, but increases rapidly with degree. While the overall value of the coefficients, which include noise and signal both first decreases and then increases. It is due to the high error/noise power at higher degrees and diminished signal power at higher degree. The signal follows the inverse law, wherein the signal power decreases as the frequency increases, and the noise follows square law wherein the noise power increases with the exponent of 2 with frequency. After degree 25 the signal power shoots up unexpectedly, this limit is denoted by a green line in figure. The error matrix provided along with the data are the monthly errors estimated in the Stokes coefficients. We define GRACE errors as the total error in the monthly gravity solutions, caused by a combination of measurement errors, processing errors, and errors in the geophysical models. Now we

require residual spherical harmonic coefficients for getting the mass change. And the residuals are dominated by errors for degree n greater than 15. The spatial resolution depends on the spherical harmonic degree terms used, they are related to each other (John Wahr [2004]).

$$S = \frac{20000}{n} \tag{3.14}$$

So if we just consider terms up to 15 degree we would be having poor spatial resolution of 1333.33 km and if we go for including higher degree term we need to take care of noise, hence we require filtering. In this thesis work we used up to degree 60 term which gives a spatial resolution of 333.33 km. Also the GRACE coefficients are good in along track direction which is north-south and thus we have poor sampling in east-west direction which is also responsible for north-south stripes in gravity maps (Bentel [2009]).

3.3 Residual coefficients and truncation

Since as per the relation we need ΔC_{nm} and ΔS_{nm} to get the density change. The data set used by us is provided by GFZ, static gravity potential coefficients C_{nm} and S_{nm}. So, we should take mean of the coefficients obtained so far in the data set and then subtract the mean to get the residual coefficients also called anomalies. This method would not yield good results if we take whole data set for mean computation (not integer number of years), since the seasonal effects are not taken into account (Oliver Baur [2011]). To prevent aliasing effect of strong seasonal signal from affecting our time series analysis we take complete integer number of years to get the mean value of data, we calculate the mean for the static gravity field represented by the spherical harmonic coefficients data set for the time period from March 2004 to February 2011. The mean is better if we take more number of years but the data set available without data gaps to us is in this time frame only.

This mean matrix obtained of size 121×121 is then subtracted from every monthly data set of same dimension. The result is called residual spherical harmonic coefficient for each month which represent the gravity potential anomaly. The residual data set contains ΔC_{nm} and ΔS_{nm} which are required for getting the mass changes as per the mathematics discussed in this chapter earlier. The data now we have consists of monthly residual spherical harmonic coefficients up to 120 degree. We need only up to 60 degree terms for the spatial resolution we want to achieve, so we truncate the matrices to 61×61.

This residual coefficient data set is noisy hence we need to apply filter to this data set. Filtering of spherical harmonic coefficients is different from filtering used in image processing. Filtering is discussed in the next section.

3.3.1 Filtering

Filtering is a method of suppressing noise in the data. White noise is generally random in nature because of which the data behaviour is not smooth thus after filtering we get smoother data. Filtering is an operation on a signal that changes the spectrum of the signal. A filter is a device (or a computer program) which applies such a change to a signal. The common filters known are Mean filter, Mode filter, Median filter, Gaussian filter, De-striping filter, Fan filter, Butter-worth filter and so on.

To remove noise we should first of all look into what comprises these errors. Various known time-variable gravity effects are already reduced from GRACE data in the course of the parameter estimation process. These effects are that from third body accelerations on the satellites and the earth, due to the gravitational pull from sun. The effect of moon and planets, the luni-solar tides of the solid Earth, the ocean and the atmosphere, gravity variation from short term (non-tidal) mass redistribution in the atmosphere and the oceans, secular gravity changes in selected long-wavelength gravity coefficients due to the global isostatic adjustment as well as the pole tide effect on the solid earth and the oceans caused by the variation in the earth's rotation (Flechtner [2010]). So in principle the GRACE monthly data should represent the unmodeled effects such as from hydrology, post glacial rebound, mass changes in the polar ice cap, earthquake and volcanic activities of higher magnitude as post seismic deformation. In addition to unmodeled effects, also spurious gravity signals from unwanted systematic and random contributions are present in the data. These arise from various sources ranging from potential deficiencies in the GRACE instrument data, in the parametrization of the orbital motion, GPS errors, to errors in the background models that have been accounted for as stated earlier. These errors along with limited sampling in east west direction and limited sampling in time domain contribute significantly to correlated errors of GRACE gravity data. The effects of such spurious gravity signals can be reduced significantly by filtering of GRACE spherical harmonic coefficients either by isotropic or non-isotropic filtering technique.

Typically filters are classified in to isotropic and non-isotropic filters. Isotropic filters

are those who behave same in every direction, or in other words they do not depend on orientation. While the non-isotropic filter is direction/orientation dependent (Jekeli [1981]). Gaussian filter is an example of isotropic filter and de-striping filter is an example of non-isotropic filter.The filtering is thought of in spatial domain but doing it in spatial domain is tough since it is convolution of the transfer function of filter with that of signal/data. In spatial domain ideally we have spherical earth; it is tough to design a filter for portion of spherical surface. Averaging gravity anomalies over a spherical cap is a typical operation in isotopic filtering. While, when mean anomalies are viewed as averages over spherical blocks (trapezoidal) delimited by convenient global or local curvilinear coordinate lines we have non-isotropic filtering in use. Since spectral theory says that convolution in spatial domain is equivalent to multiplication in spectral domain we prefer to do it in spectral domain (Jekeli [1981]).

We would use Gaussian 500 km radius filter for our data because the spatial resolution of the data set is around 400 km and we can get the proper smoothing if we keep filter radius greater than that otherwise the filter would be ineffective. Gaussian filter is a type of averaging filter, this type of filtering technique is simple and effective. Although people are doubtful about its performance as it is simple and isotropic and the GRACE noise itself is not isotropic. But it is satisfactory when it comes to execution and result quality for the application we are interested in. An isotropic filter has weight depending only on the SH degree n, and hence wavelength, but not on the orientation. It has a bell shape spectral spread which would select the coefficients under the bell and weight them according to their distance from central value in our case it is $n = 0$, $m = 0$. So larger the order and degree least is the contribution of that coefficient. The Gaussian spatial averaging, an isotropic filter given by John Wahr [1998] is used in this work. It is given by:

$$W(\alpha) = \frac{b}{2\pi} \frac{exp(-b(1 - \cos \alpha))}{1 - \exp^{-} 2b} \tag{3.15}$$

$$b = \frac{\log(2)}{(1 - \cos(\frac{r}{a}))} \tag{3.16}$$

where r is the averaging radius. The behaviour of this isotropic filter in frequency domain is shown in figure 3.3 for different averaging radius.
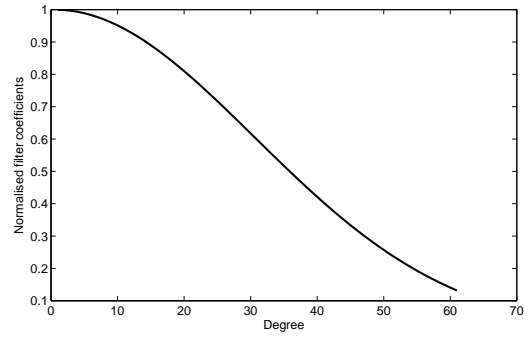
(a) Spectrum for averaging radius of 250 km
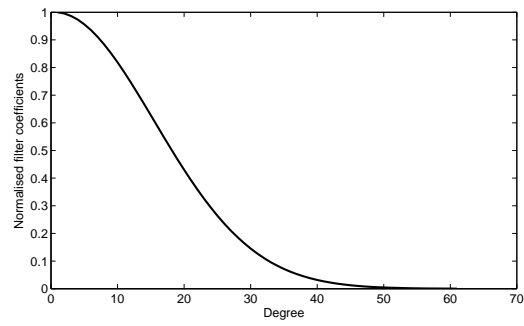
(b) Spectrum for averaging radius of 500 km
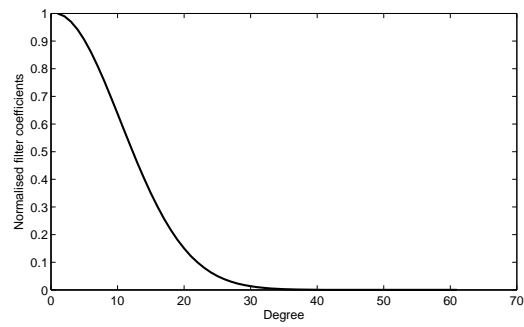
(c) Spectrum for averaging radius of 750 km
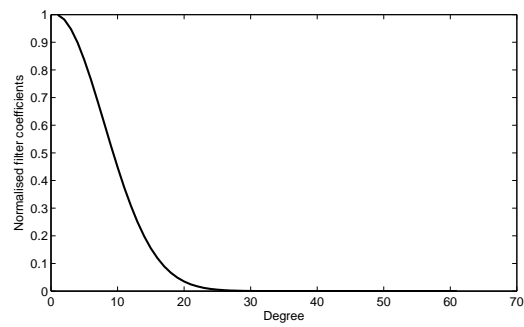
(d) Spectrum for averaging radius of 1000 km

Figure 3.3: Gaussian filter spectrum

The Gaussian filter spectrum for different averaging radius illustrates that as we increase the radius the weight allotted to the higher order coefficients decreases and we are left with more of lower order coefficients in our filtered set of data which are less noisy.

The question pops up here is how these coefficients are converted to quantities such as gravity anomaly, geoid height, Equivalent Water Height (EWH) and how is the interpretation done thereafter.

3.4   Interpretation

The GRACE data accounts for all the mass changes which took place at a location irrespective of in which layer the change occurred. Thus we are not able to separate layers unless and until we have other ancillary data. While analysing the data and representation of mass distribution we can consider that change is taking place at an hypothetical surface layer. We can replace integral by mass layer of constant thickness h.

$$\int_r \delta\rho(\theta_Q, \lambda_Q, r_Q) \frac{r_Q}{a}^{(n+2)} pr_Q \cong \Delta\rho(\theta, \lambda)h \tag{3.17}$$

So now we have density change multiplied by height which can be represented by density of water multiplied by height, known as equivalent water height. We use equivalent water height because the major contribution to time-variability of local gravity field after removing atmospheric and ocean is hydrology. But,we can represent this surface layer change in terms of height of rock, and ice just we need to replace the density and we get the height. Which is just a representation.

Water is having the least value of density that is $1000 \, \text{kg}/m^3$ amongst mean density of Earth, rock, and ocean which are $5517 \, \text{kg}/m^3$, $2670 \, \text{kg}/m^3$, and $1027 \, \text{kg}/m^3$ respectively. Thus, when we talk of equivalent water height the magnitude height is amplified by factor of ratio of the density of material and the density of water. Also, Earth is considered to be perfectly elastic body so if there is a mass change, which would mean that mass is either added or removed upon the earth body, then the earth goes under deformation showing the strain due to the stress produced by the mass change. This change in earth body should also be included when we study them with GRACE data. To represent this elastic effect we have love load numbers introduced in the spherical harmonic coefficients expansion in term of density

change given by a scientist and the name Love is after his name A.E.H.Love.

The value of love load number is fixed and depends on the degree. For example for degree $n = 0$ k_0 is 0 since the total mass of solid Earth and its fluids is constant, mass of single fluid is not constant and variable atmosphere and ocean does not cause deformation of solid Earth. For degree $n = 1$, we know that ΔC_{10} ΔC_{11} and ΔS_{11} are proportional to position of Earth's centre of mass relative to centre of coordinate system, so the degree 1 components should not vanish but their sum should, so $k_1 = -1$. If the origin is taken as centre of figure of solid Earth then $k_1 = +0.027$ (off-set between centre of mass and centre of deformed figure).

Gaussian 500 km radius filter is applied to the residual coefficients. We get the time-series of global gravity maps as output. The EWH maps from year 2005 for the month of January, April, August, and December are shown in figure. The Root Mean Square (RMS) of EWH maps generated is found to be 1.63 cm. RMS is a statistical measure of the magnitude of a varying quantity.
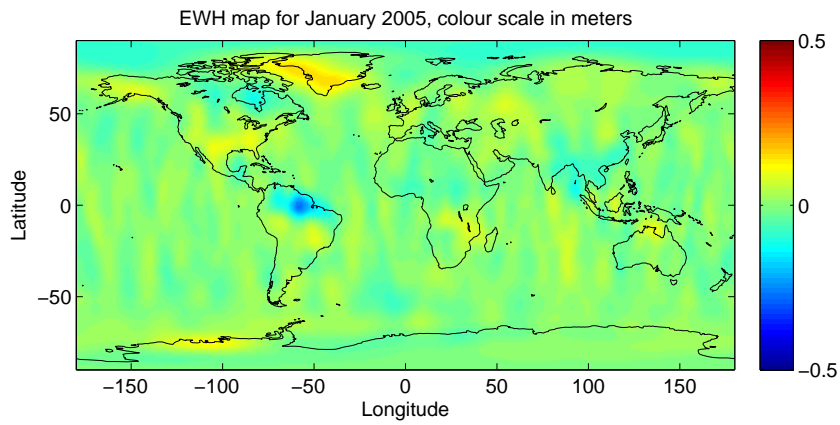
(a) EWH global map for January 2005
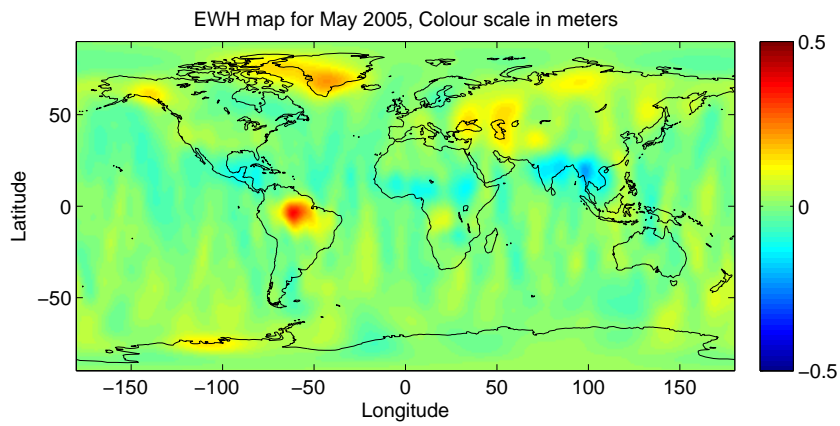
(b) EWH global map for May 2005
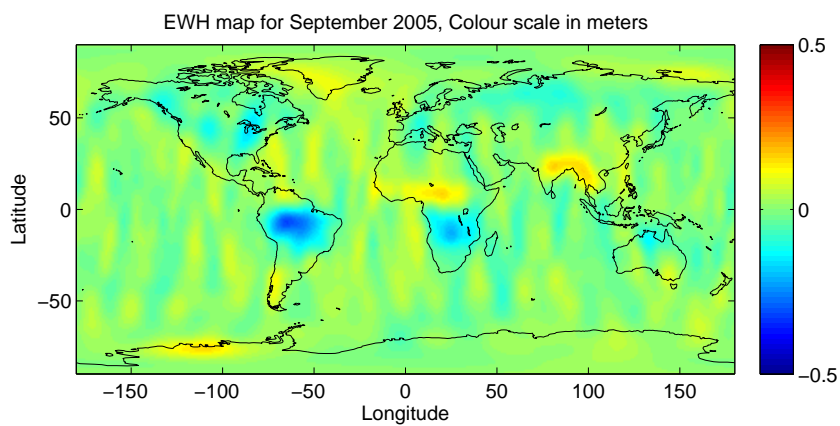
(c) EWH global map for September 2005

Figure 3.4: EWH global map for different months of year 2005

In next few chapters we would discuss about various events which we look forward to observe in GRACE data set. We are going to investigate the major limitations about the GRACE observations and the points which we need to keep in mind while analysing GRACE data for a particular event would be highlighted. The time series plots and residual plots are analysed to indicate the major events. We would start with hydrological events mainly floods and droughts in major river basins across the world. Then we would look for major earthquakes events followed by analysing volcanoes by trend analysis and finally with few glaciers showing also by trend analysis.

All these events induce gravity change either periodic, continuous or sudden. Earthquakes have a sudden jump in signal, volcanoes pushing earth surface and glaciers receding have trend while hydrology show up periodical mass fluctuations, which we can see in coming chapters.

Chapter 4

Hydrology

4.1 Introduction

Water is one of our, most important natural resources. Hydrology has evolved as a science in response to the need to understand the complex water system of the earth and help solve water problems. Hydrology is the science that encompasses the occurrence, distribution, movement and properties of the waters of the earth and their relationship with the environment within each phase of the hydrological cycle. Major civilizations have dwelled along some river basin since water is as important as air for human beings. These basins have annual cycle of hydrological mass changes. These mass changes can be seen as GRACE positive or negative EWH calculated from spherical harmonic coefficient residuals. These mass movements might be due to Ground water storage along with Surface water mass or soil moisture. GRACE cannot separate layers so we need to use hydrological models to separate different layers.

The two major hydrological applications where researchers have found GRACE extremely motivating are ground water storage change estimation and calibration of global hydrological models (J. Riegger [2010]). Many studies for the ground water depletion have been done. Work done by Mathew Rodell [2009] shows that GRACE and simulated soil-moisture from a data integrating hydrological modelling system, shows that ground water is depleted at a mean rate of 4.0± 1.0 cm per year over the Indian states of Rajasthan, Punjab and Haryana (including Delhi). Similar type of analysis with GRACE data, monitored well-network observations, and GLDAS obtained soil moisture was done for Mississippi river basin by Mathew Rodell [2006]. Walter W. Immerzeel [2010] worked on how the climate change

would affect the flow of water in the major Indian River basins. The effects of 2003 European heat wave were investigated by Ole B. Andersen [2005]. He validated GRACE results with terrestrial superconducting gravimetric data, although the density of gravimeter data is not good and also not evenly distributed but was enough to make up with GRACE resolution. People have discussed GRACE observed water mass redistribution along with other hydrological models and ancillary data to conclude that GRACE is a potential mission for hydrological research.

The GRACE observed gravity changes are over a spatial scale of 400 km. So, large basins can only be monitored by GRACE. The Amazon basin is considered the largest hydrographic river basin in the world with 6.1 million square km, extending from the Andes to the Atlantic Ocean. The large range of annual water level variations from season to season can be seen in GRACE, in fact the Amazon signal is the largest signal observed by GRACE. The GRACE observed EWH were found to be in high correlation with measured river levels at more than 230 locations in the Amazon basin. The ground water variation is correlated with river water time-variations in central sedimentary basins (Flavio Guilherme Vaz de Almeida [2012]).

In this thesis work we try to observe floods and droughts in the GRACE observed time variable gravity. These two events pose a great amount of threat to food and life security to mankind. Floods and droughts are among the most dangerous and costly of all natural disasters. According to statistics from the United Nations, during 1970-2005 over 30% of natural disasters were floods and nearly 15% were droughts or drought-related (wild fires and extreme high temperatures). During the 30-year period 1980-2009, floods accounted for more deaths in the United States than hurricanes, tornado or lightning, ranking first among weather fatalities. Droughts are the main cause of agricultural distress, accounting for over $11 billion in damage in the United States during the first decade of this century. There are numerous ways to define or categorize both floods and droughts (Dirmeyer [2011]).

Meteorological floods and droughts are classified based on anomalies in precipitation. Hydrological floods and droughts are measured in terms of deviations of stream-flow or river water depth from historical norms. Agricultural floods and droughts are defined by their impact on crops and livestock. Other more specialized stake holders such as dam and reservoir operators, hydroelectric power concerns, river transportation networks and municipal water managers, to name a few, have their own criteria for defining floods and droughts. We will speak here primarily in terms of meteorological extremes based on anomalies from

climatological annual cycles of precipitation.

GRACE is able to see the storage change, which was demonstrated by Florian Seitz [2008]. They investigated the hydrological mass variation due to extreme weather conditions in central Europe. The time series produced by him was validated by independent results from atmospheric and hydrological data. We took this as the basis to conclude that other basins and event would eventually follow the agreement with GRACE. The interpretations drawn out from time-series and residual plots were in agreement with the events reported to occur in various major river basins.

4.2 Analysis tools and strategy

We would use time series analysis and generate residual plots further to investigate the two hydrological events. So, first of all we start with short introduction about time series analysis followed by the discussion about residual plots and how they are generated. Their importance in the analysis, with the major considerations we have to take into account while their generation and interpretation will also be discussed.

4.2.1 Time series analysis

A time series is a sequence of data points, measured typically at successive time instants spaced at uniform time intervals. The main objective of time series analysis is identifying the nature of the phenomenon represented by the sequence of observations. A time series model will generally reflect the fact that observations close together in time will be more closely related than observations further apart. The analysis could be carried out in spectral or temporal domain, we chose temporal domain.

Time series generation in our case would be to place the EWH obtained from post-processing of GRACE monthly residual spherical harmonic coefficients. We would consider the monthly gaps in time series plots. These time series show annual signal as sinusoidal curve for large basins such as Amazon or Congo. The seasonal cycle is very prominent and for searching floods and droughts we would observe outliers in the time series, these outliers might appear due to noise or only due to terrestrial water storage change or due to flooding or drought events. These things are difficult to comment on unless we have some ancillary in-situ data to separate these phenomenons seen together by GRACE. The flood and drought analysis is

not simple. We have to take care of other factors, such as duration of flood or drought, their spatial extent and magnitude of the event, which affects the quality of results. The time series alone is not enough because when we talk of regional scales of big basins, these events carrying small signal relative to basin extent signal may not appear significant. Also the systematic behaviour of time-series would make the outliers small in magnitude undetectable visually. So we have to check residuals of the time series generated to make the deviation from mean behaviour visible by a significant amount and to take care of systematic behaviour of time-series. These problems with time-series would be demonstrated and pointed out in the section of floods later in this chapter.

4.2.2   Residual plots

Residual denote the deviation from the mean behaviour of time-series. Residual of a time series would tell us how the things have varied with respect to a long term mean. To account for systematic behaviour of time-series data we must identify trend and then de-trend it before calculating mean. In our case we took the mean of integer number of years to avoid any seasonal bias. Gaps in data cannot be included while computing mean so the time period when GRACE was healthy and we have continuous data was opted. The time period from February 2004 to January 2009 is chosen to get the mean of de-trended time-series for residual calculation. These residual plots indicate sudden deviation for the time period when these floods and drought events occurred. We have to be careful when we say that whether we can see a flood or drought, and also in deciding how we can see a flood or drought more efficiently. These things are explained in the following sections of flood and droughts.

4.3   Floods

Flood is defined as overflow or inundation of water that comes from a river or other body of water and causes or threatens damage. Flood occurs when certain hydrological conditions exist at same time such as saturation in soil moisture, increased and continuous precipitation, groundwater saturation and high humidity. The precipitation alone is not responsible for floods. Hydrology is governed by the water balance equation:

While preparing time series for flood analysis the things that should be taken care of are as follows:

1. Floods occur not at the basin scale rather they are localized generally in a location nearby river only. So if we select whole of the basin, the strong signal limited to certain spatial extent would be averaged out with whole basin area signal. So the strength of signal would diminish and even might get lost. Hence, while analysing floods one should take care of the area for which the time series and residual plots are generated.

2. Secondly, the floods are not events that last for months or even few weeks in general. Floods are short -lived, lasting hours to days. Only large scale floods can last weeks or months and such floods are rare. Since the GRACE solutions are monthly so if we have a flooding event for a week it would be averaged over month so in that case also getting strong signal for flood is tough job. The floods which result after regular or continuous precipitation resulting into saturation in soil moisture and water table, and later submerging of surface would appear as distinguished peak, although such flood would prevail few days but the mass change introduced is significant. The spatial extent of flood activity plays a vital role since the spatial resolution of GRACE is a major limitation in analysis of events causing mass change. Thus large scale floods can be seen clearly in GRACE data set.

4.3.1 Methodology used and analysis of various flooding events

The steps involved in the flood analysis are enumerated below:

1. We prepare a list of all the major floods throughout the world in the years for which we are analysing the GRACE observed local gravity variations, we also get the duration and area affected by a particular flood. We used the data from "flood archive" issued for every year by Dartmouth flood observatory.

2. Next, we locate the area and define the coordinates which would cover maximum area under flood. For the case when we have a very large scale flood which covers nearly whole of the basin taking basin scale time-series is beneficial and we found two such flooding events in the time frame we are interested in. One is the 2009 Amazon floods and second is 2010 Pakistan floods.

3. For the grid under observation defined by the latitude and longitude, we take mean of the EWH values of every $1° \times 1°$ pixel in the grid. The mean for every month is

calculated and represented in the time-series as individual points. Then we generate the residual plot for the same area by following the methodology discussed in the section residual plot.

4. Observe the time-series, if the flood occurred in the rainy season then since every year we get the water level rise in the region in that part of year, the annual GRACE cycle would be giving a peak every time in that part of year. So, we would get a distinguished peak due to a flooding event among peaks, for the month when floods were reported. If the flood occurred in the dry season or any season other than rainy then searching peaks in the time-series is not a good idea rather the depression in annual cycle observed every year would appear less low for the month for time frame in which the floods are reported. In the case discussed later residuals are very helpful since they describe the anomalous behaviour from the mean behaviour and floods would always appear to be a peak while analysing them.

We would analyse large floods which occurred after 2002 and before 2011

1. 2009 Amazon flood

   Amazon River basin experienced flood in the year 2009. It was large scale flood spread over a large area and for time period of more than a month. For this case instead of selecting few regions we should take whole basin. we can observe a peak in time-series of EWH plotted in the year 2009. The team of J.L. Chen also did a work on analysing extreme weather condition by GRACE, they studied Amazon 2009 floods and associated it with the terrestrial water storage as a parameter to comment on the condition during floods (J. L. Chen and Tapley [2010]). The basin map of Amazon is shown in figure 4.1.

Figure 4.1: Amazon basin map, the yellow region shows the basin cover

Observing the time series plot of EWH in figure 4.2 we can see a annual cycle. These cycles when have outlier for any instant we can expect some event. For flooding event the outlier has to be a maximum. we observe a peak more than normal peaks for corresponding time in different years. In 2009 we observe maximum peak which is the time of flooding.
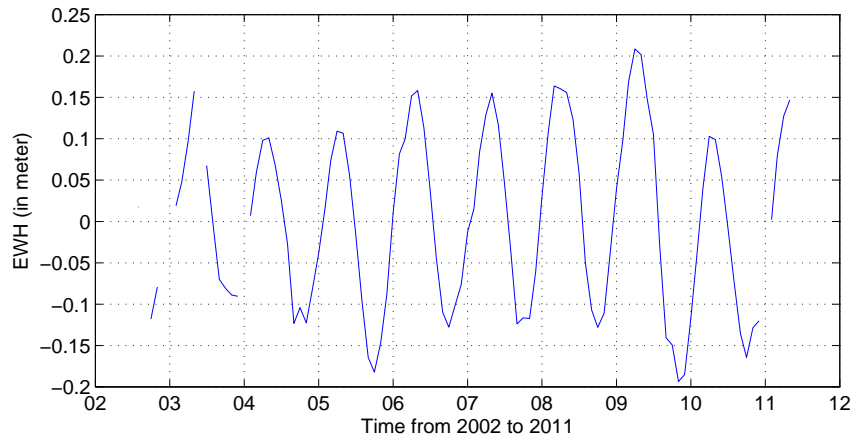
Figure 4.2: Times-series plot of EWH for Amazon basin

The residual plot in figure 4.3 also shows a distinguished peak for 2009 flooding event.
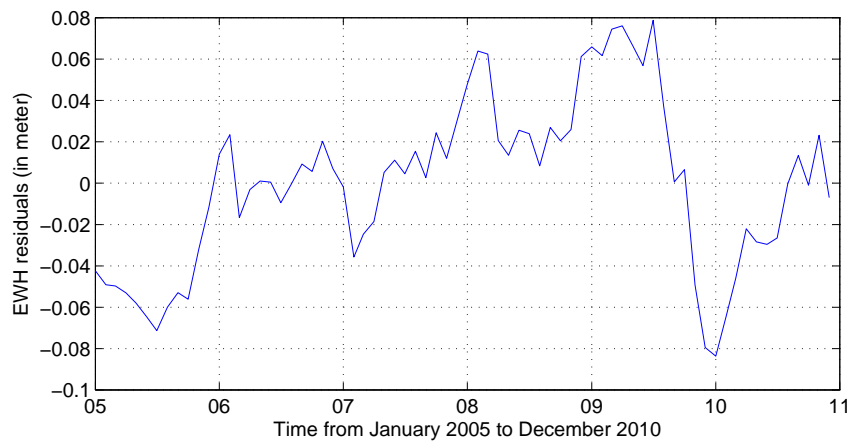
Figure 4.3: Residual plot for Amazon basin

2. 2004 Flood in Sao Paulo

Sao paulo is a province in Brazil. In 2004 Sao Paulo and neighbouring region experi-

enced large flooding (Schmidt and Coppola [2012]). We investigated for Parana river basin in Sao paulo for this flooding and the time-series of equivalent water height and its residuals showed no sign of any outlier describing floods.
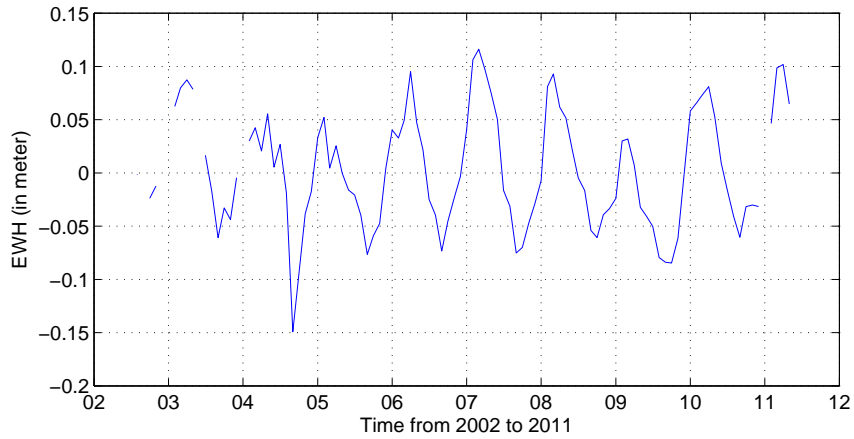
Figure 4.4: Time series plot of equivalent water height for Parana river basin
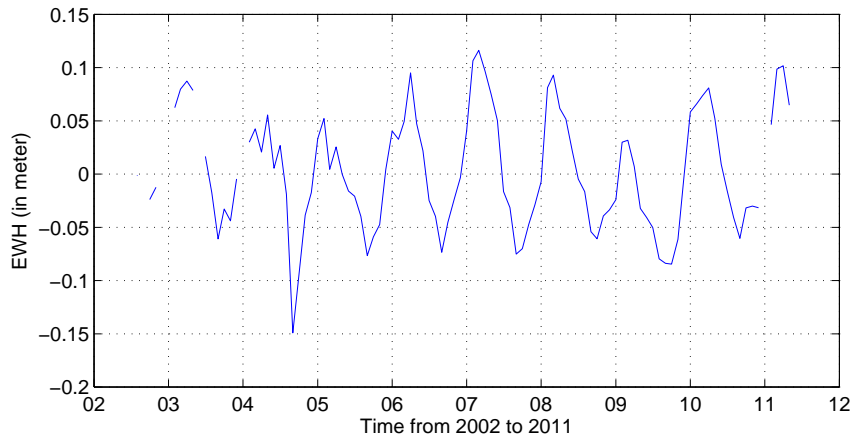
Figure 4.5: Residual plot for Parana river basin

But when we select the region for Sao Paulo only we get the strong outlier in 2004. We selected a 4 degree× 4 degree grid covering Sao Paulo and surrounding regions as shown in figure 4.6. We can see this flooding event in time-series and residual plot of

41

EWH further.

Figure 4.6: Selected area for Sao Paulo flood analysis

We were able to see the peak in the time series plot and residual plot as well for the region selected.
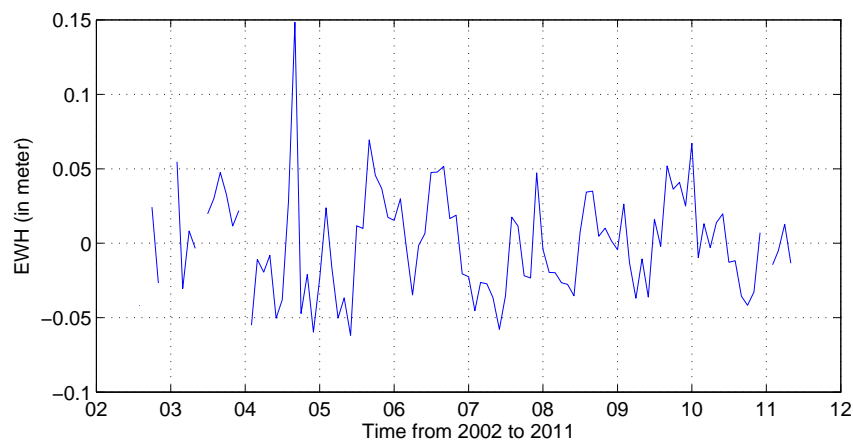
Figure 4.7: Time-series plot of EWH for Sao Paulo region

The residual plot also indicates a large mass change in 2004.

42
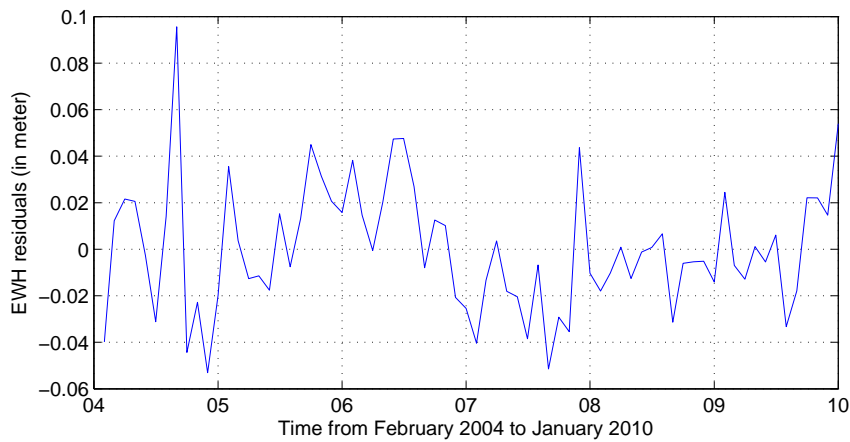
Figure 4.8: Residual plot for Sao Paulo region

3. 2004 China flooding

   This flood in the month of September lasted for more than 15 days and is considered to be one of the most deadly floods occurred in China. The death toll was 196. This flooding event is not visible in the time series and residual plot. The area affected by floods was 72,280 square km. The possible reason could be duration of flood which was mere 7 days (200 [2005]). The floods affected mainly the Sichuan Province and Chongqing Municipality along Zhou River, Upper Yangtze (above Three Gorges Dam). the selected region for analysis is shown in the figure below:

43
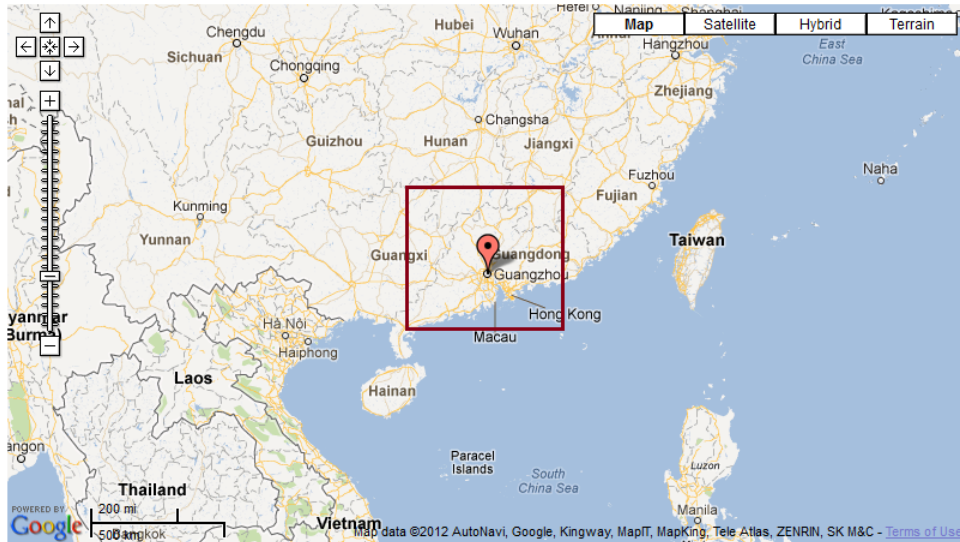
Figure 4.9: Area selected for analysing China 2004 flooding

The time-series does not shows any signal of significant mass change which shows sign of floods.
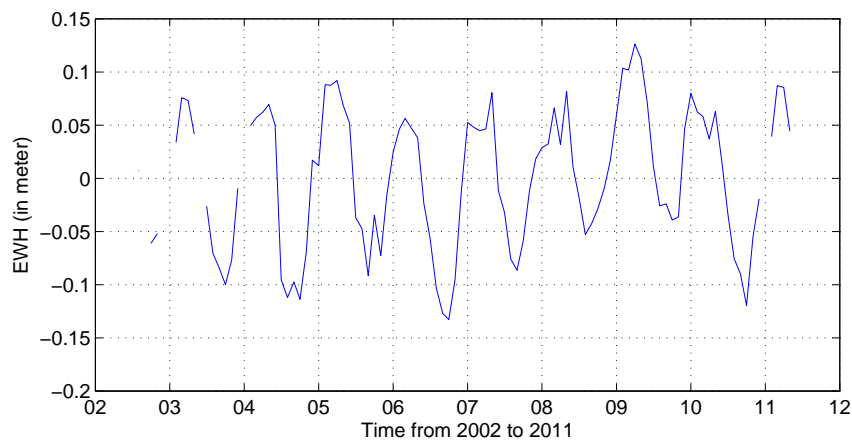
Figure 4.10: Time-series plot of EWH for China 2004 floods

The residual plot is also unable to show any flooding event.
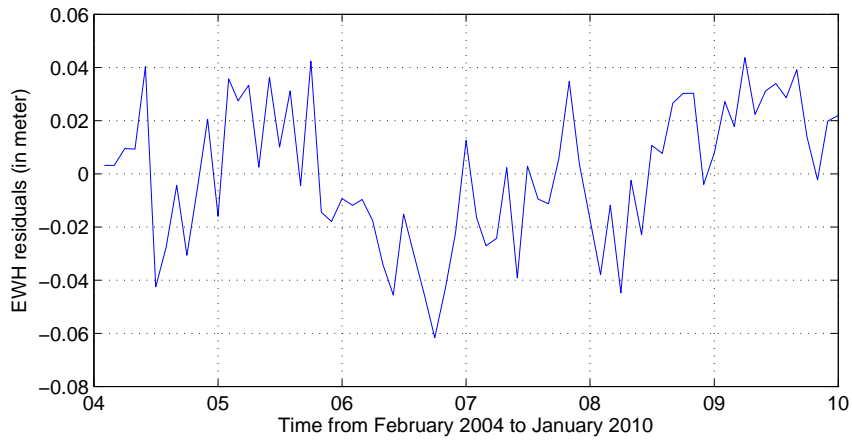
Figure 4.11: Residual plot for China 2004 floods

4. Mumbai and surrounding region 2005 monsoon floods

   The monsoon in India could be very severe at times, it caused floods in Mumbai and surrounding region due to Sudden outburst of rains. 2005 floods took 1053 people's life and it was on large spatial scale covering up to a neighbouring state Karnataka (200 [2006]). This is visible in GRACE observed EWH, most pronounced in residuals. We took a large area of 4 degree× 4 degree grid as shown in figure 4.12.

Figure 4.12: Area selected for Mumbai, India flooding 2005

The time-series of EWH shows a small peak in the year 2005.
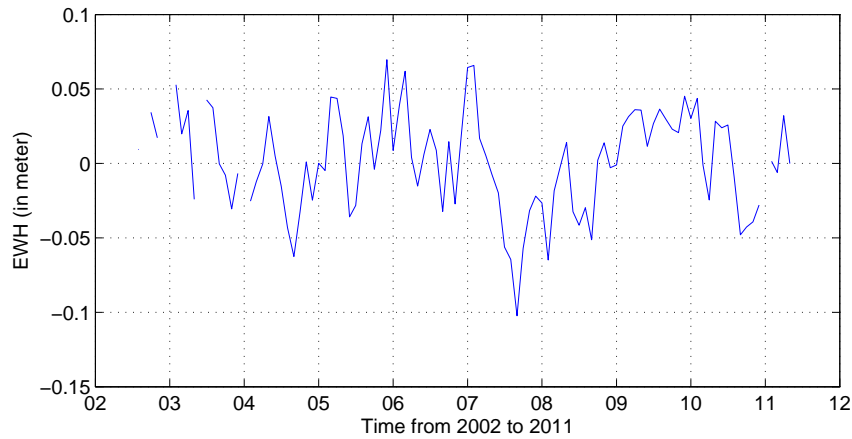
Figure 4.13: Time-series plot of EWH for Mumbai and surrounding region floods 2005

The residual plot shows this flooding event even better than time-series.

46
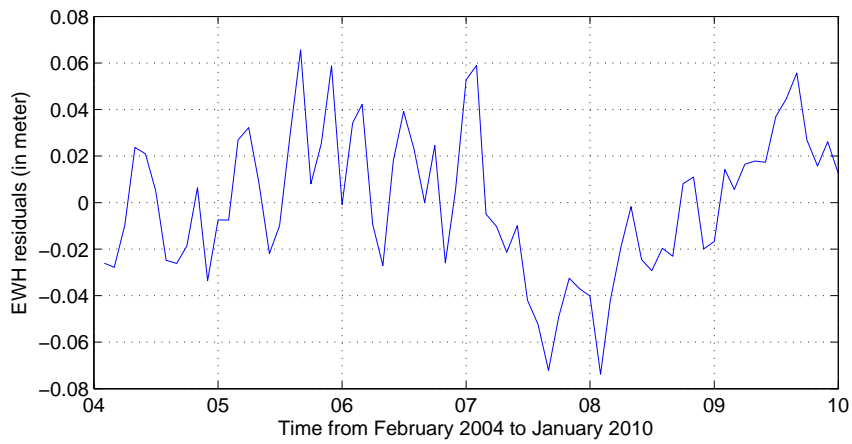
Figure 4.14: Residual plot for Mumbai and surrounding region floods 2005

5. China Fujian floods 2005

They are visible in GRACE data set. The residuals are exceptionally positive for the whole year. Death toll in this flood was 111 and it lasted for 5 days (200 [2006]). The selected area for analysis is shown in figure 4.15.

Figure 4.15: selected region for Fujian flood analysis

47

The time-series shows a peak in 2005.
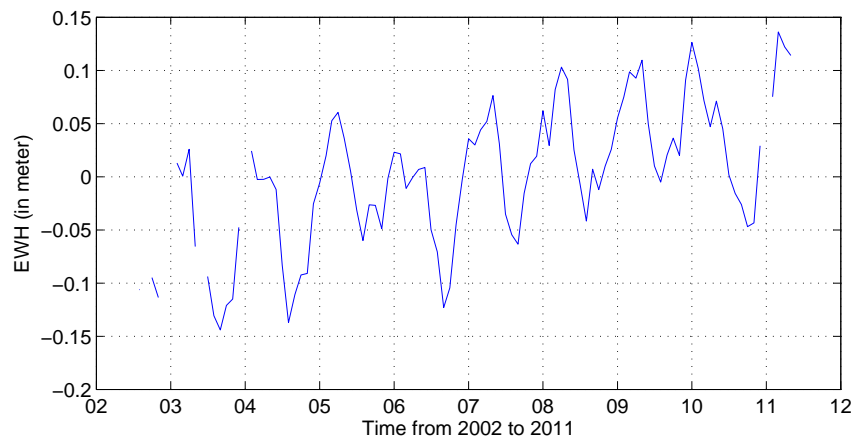
Figure 4.16: Time-series plot of EWH for Fujian flood analysis

The effect is more pronounced in the residual plot.
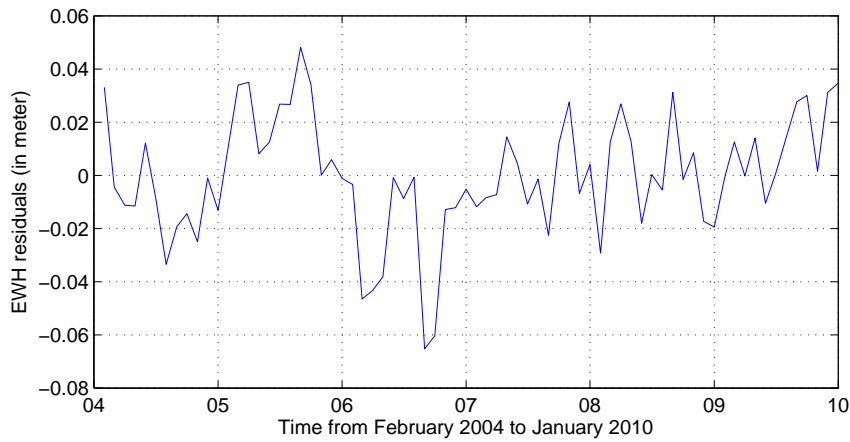
Figure 4.17: Residual plot for Fujian flood analysis

6. New Orleans 2005 and 2009 floods

The hurricane in August with heavy rainfall was responsible for floods which lasted for 22 days but was covering small area, and thus the sudden small signal peak in August is seen in residuals but not significant for 2005 floods (200 [2006]). While, the 2009 floods by hurricane Katrina was large in terms of mass of water involved in floods and the time period for which it affected the area.The 2009 floods show up as high peak in the residual plots, while the time-series did not showed the flooding events as an clear outlier, the reason is presence of a systematic signal (trend) due to subsidence of city. This would be explained further, the region selected is shown in figure 4.18.

49
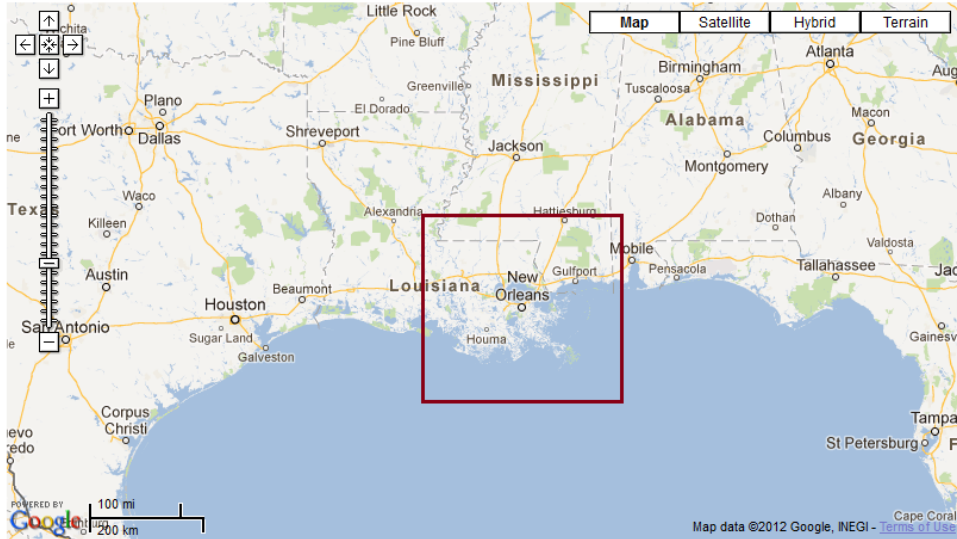
Figure 4.18: Selected region for analysis of New Orleans flooding events

Time series showing a trend thus the outlier is present but visually it seems to be suppressed, this is due to the systematic behaviour of signal. The flooding peak is substantially lower than the previous normal annual cycle peaks due to presence of trend, which is due to subsidence of city. This can be seen in figure 4.19.
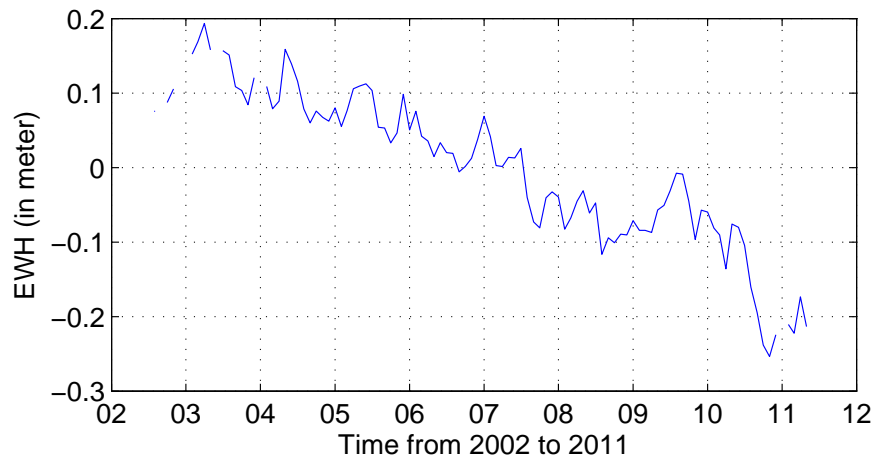
Figure 4.19: Time-series plot for New Orleans flood analysis

In residuals calculation first we remove trend from time-series and then we calculate it. Thus, the signal for flood in 2009 can be seen clearly in figure 4.20.
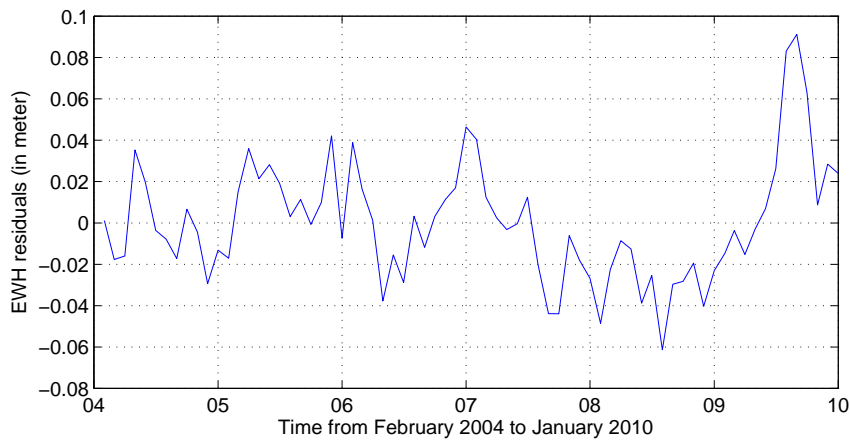
Figure 4.20: Residual plot for New Orleans flood analysis

7. Kenya Ethiopia floods 2006

Africa was under drought for about a decade had a relief in 2006 and then a normal precipitation in 2007. Kenya and Ethiopia with huge rainfall in October and November caused them to experienced floods and this event is very well seen by GRACE. The floods lasted for 60 days and covered 504,000 square km in total. Figure 4.21 shows the area selected for analysis.
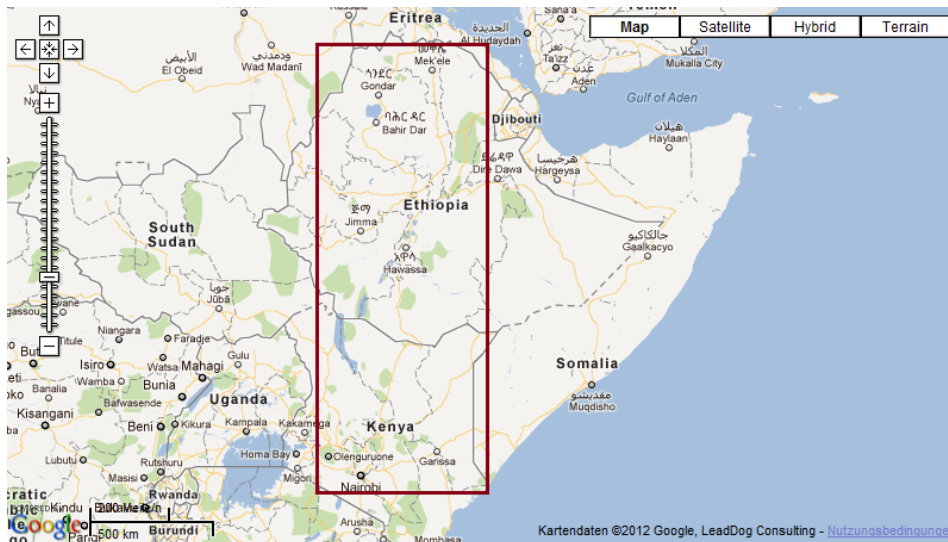
Figure 4.21: Area selected for Kenya, Ethiopia floods

Time series in figure 4.22 is showing the flood event as peak in 2006.
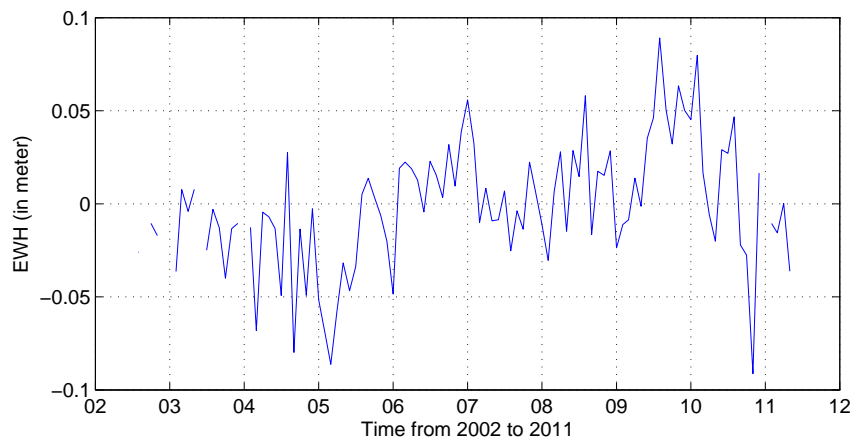
Figure 4.22: Time-series of EWH for Kenya, Ethiopia flood analysis

In residuals also shown in figure 4.23, the signal (high value of EWH) for flood in 2006 can be seen.
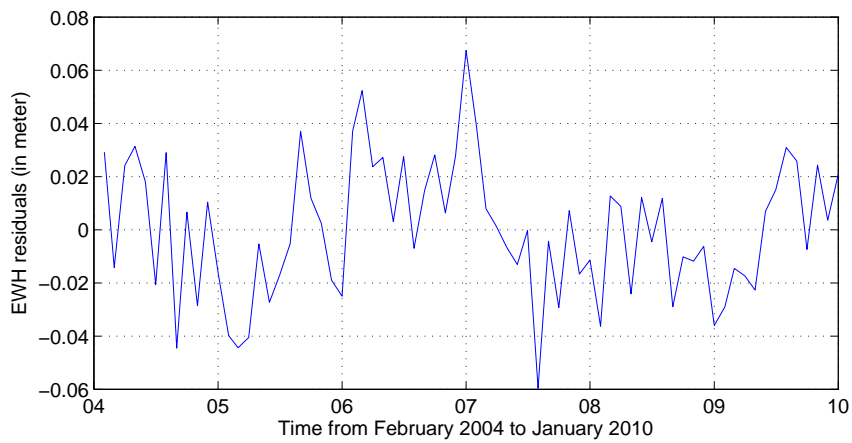
Figure 4.23: Residual plot for Kenya, Ethiopia flood analysis

8. North Korea floods 2007

The north Korean floods are not visible in either time series or residuals. The reason is not clear since the flood lasted for 18 days and covered an area of 29,480 square km (200 [2008a]). The possible explanation for such an observation is that the extent of flood was along a length and the spread was not proper. The selected region for analysis is shown in figure 4.24.

Figure 4.24: Area selected for North Korea Flood analysis

Time series in figure 4.25 shows no outlier to support the flood event in 2007.
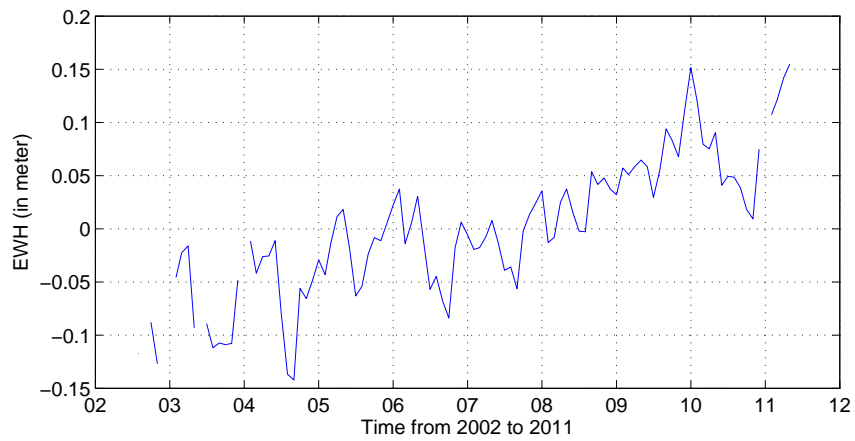
Figure 4.25: Time-series plot for North Korea Flood analysis

In residuals also there is no outlier signal for flood in 2007.
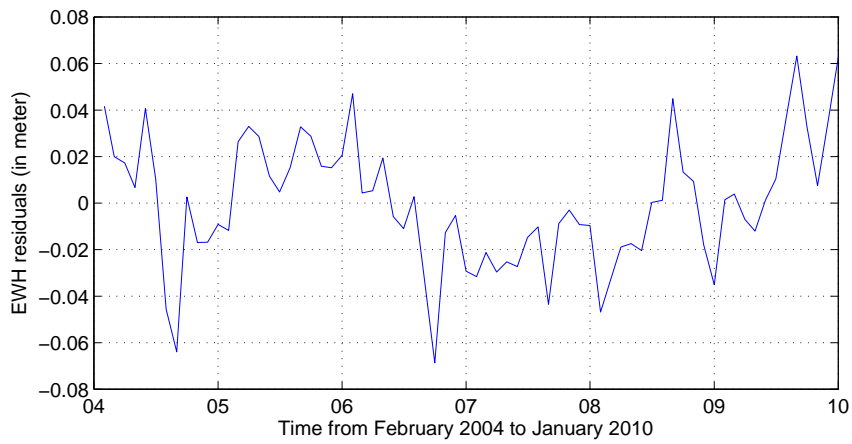
Figure 4.26: Residual plot for North Korea Flood analysis

9. Nigeria Ghana and other African nations floods 2007 September

   This is also not visible because for many of the GRACE observed years African nations have experienced drought, in 2006 they experienced heavy rainfall most probably enough to refill the terrestrial storage and replenish the soil moisture. In 2007 they had rainfall and floods for 79 days (200 [2008a]). But the amount of variation shown from long term mean by the water change in 2006 was more than that experienced in 2007 so GRACE residuals and time series wont see these floods. The area investigated is shown in figure 4.27.

55

Figure 4.27: Selected area for African Nation Flood analysis

Time series in figure 4.28 is showing no strong outlier to demonstrate flood event in 2007. The mean EWH for that year is more than previous years and less than the following years. Also the mean calculated by us for residual estimation expects a normal rising signal in middle of year for any events leading to increase in EWH but these years show a declining signal which starts rising after mid year.
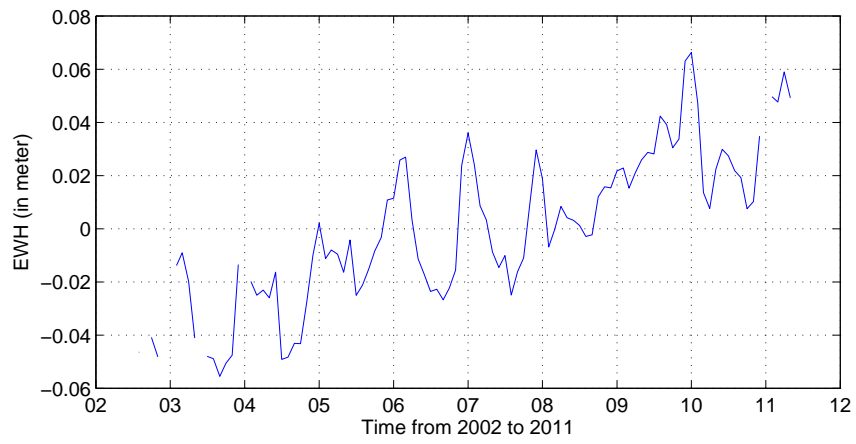
Figure 4.28: Time-series plot of EWH for African Nation- Nigeria and Ghana Flood analysis

In residuals in figure 4.29 shows no signal for flood in 2007.
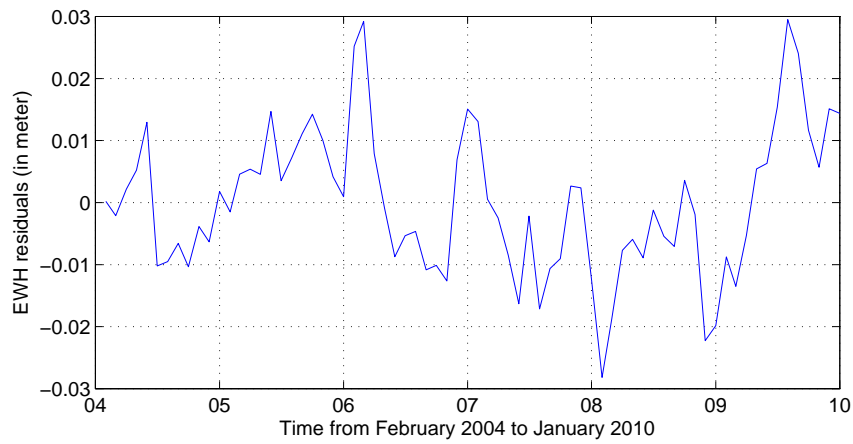
Figure 4.29: Residual plot for African Nation- Nigeria and Ghana Flood analysis

10. South China floods 2008

   It lasted for 25 days but affected area along river. It is also one of the most deadly floods seen by China (200 [2008b]). And this also is not seen in the GRACE. The invisibility of such an intense event is due to the occurrence of floods along the river length and the region is adjoining sea. The spatial extent of flood was also not large enough for GRACE.

Figure 4.30: Area selected for South China 2008 flood analysis

Time series in figure 4.31 showing no flood event in 2008.
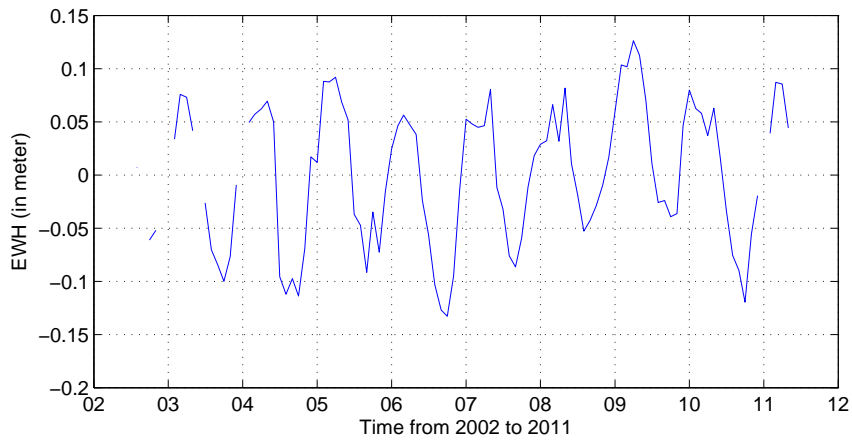
Figure 4.31: Time-series plot of EWH for South China flood analysis

In figure 4.32 for residuals, the signal for flood in 2008 can not be seen.

59
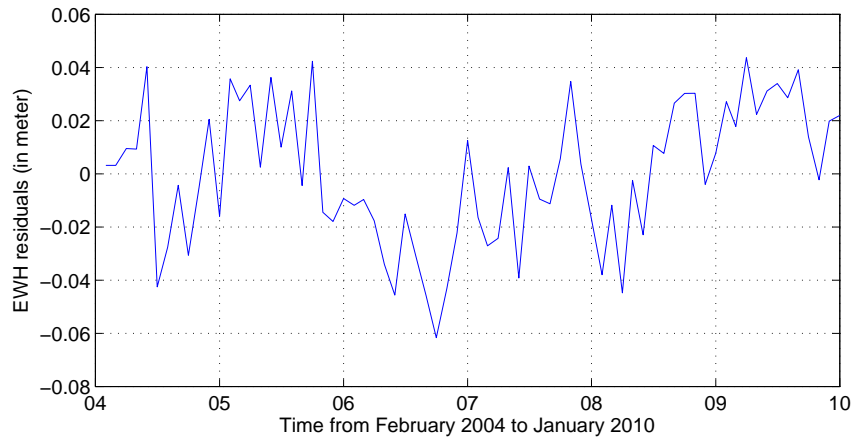
Figure 4.32: Residual plot for South China flood analysis

11. 2008 Bihar monsoon floods

In later half of the year 2008 the monsoon struck northern part of India getting maximum of the annual rainfall. Bihar, a state having Indian Rivers Ganges and its tributary Koshi river received heavy rainfall and experienced floods for 38 days covering an area of 163700 square km, and is seen by GRACE. The selected area for analysis is shown in figure 4.33.

Figure 4.33: Selected area for Bihar, India 2008 flood analysis

Time series in figure 4.34 is showing flood event in 2008 as peak but the trend in time-series makes it difficult to observe a significant peak.
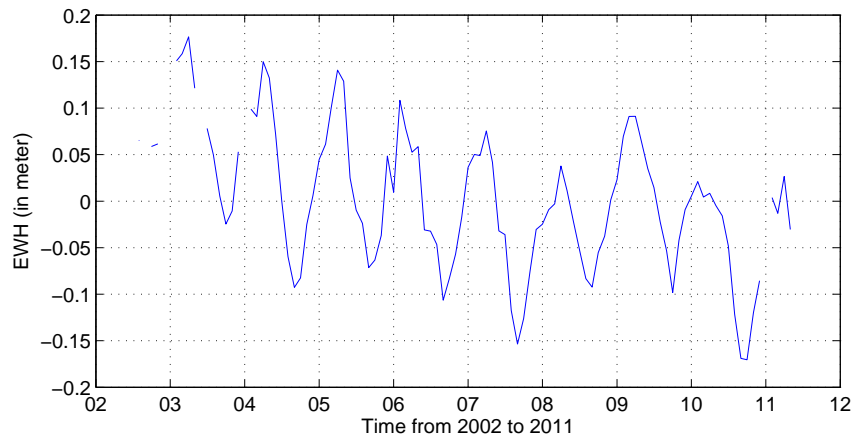
Figure 4.34: Time-series plot for Bihar, India 2008 flood analysis

In figure 4.35 the residuals shows signal for flood during 2008 clearly.
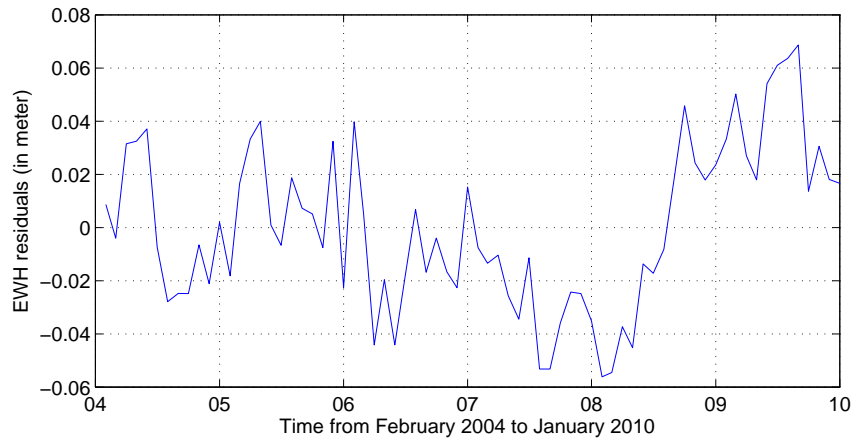
Figure 4.35: Residual plot for Bihar, India 2008 flood analysis

12. Taiwan floods 2009

This event is visible in GRACE observed EWH. Death toll was 677. This event did not covered a large area since Taiwan itself is a small country, but Taiwan received good amount of rainfall in 2008 followed by good rainfall in 2009 resulting into floods. Thus the mass was on a high for two continuous years making it a flood in 2009. The selected area for Taiwan flood analysis is shown in figure 4.36.

Figure 4.36: Selected area for Taiwan flood analysis

Time series in figure 4.37 is showing flood event in 2009 as peak.
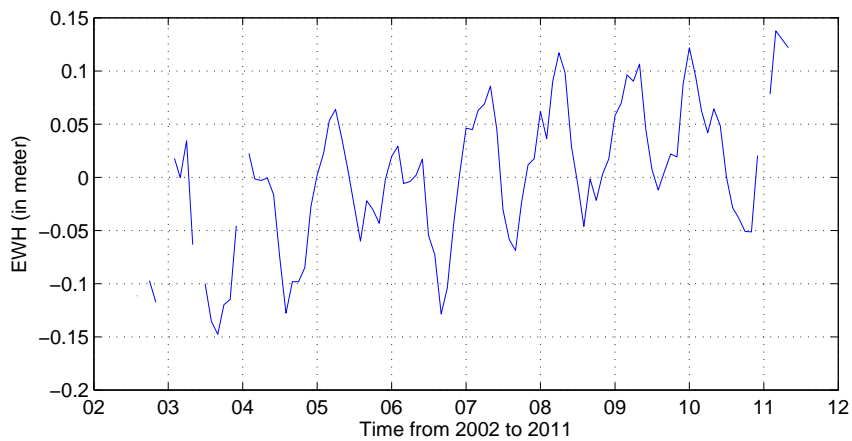
Figure 4.37: Time-series plot for Taiwan flood analysis

In figure 4.38 the residuals shows signal for flood during 2009 clearly.

63
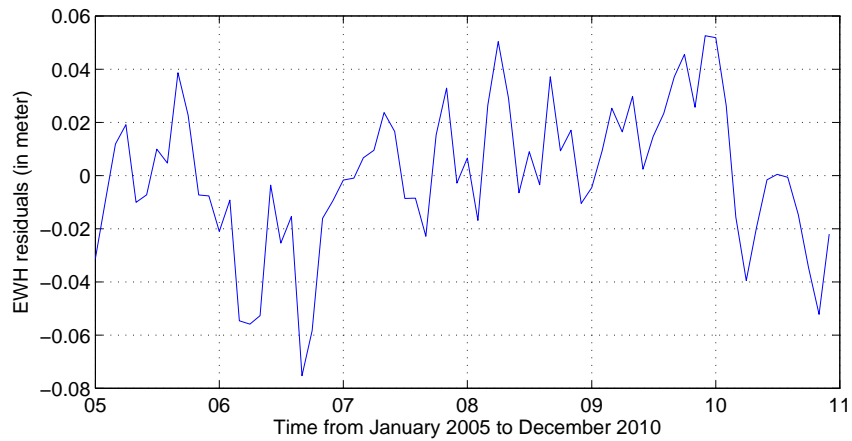
Figure 4.38: Residual plot for Taiwan flood analysis

13. Pakistan floods 2010

The flooding began in July 2010, killing at least 1,600 people, according to the UN. Twelve million were affected in Khyber Pakhtunkhwa and Punjab provinces, while a further two million are affected in Sindh. According to the federal flood commission, 557000 hectares of crop land has been flooded across the country and more than 10,000 cows have perished (201 [2010]). It is one of the major flooding events of large scale, so we went for whole basin. The basin under flood is shown in figure 4.39.
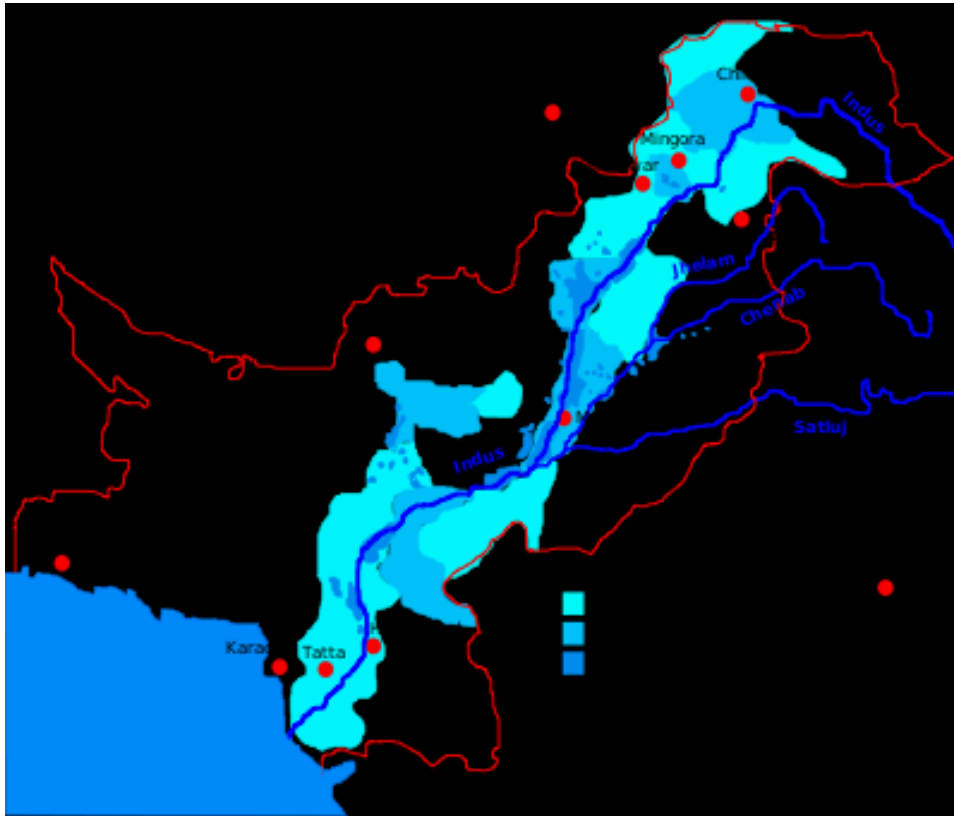
Figure 4.39: Map of Indus basin affected by floods in 2010 floods

Time series showing flood event in 2010 as peak.
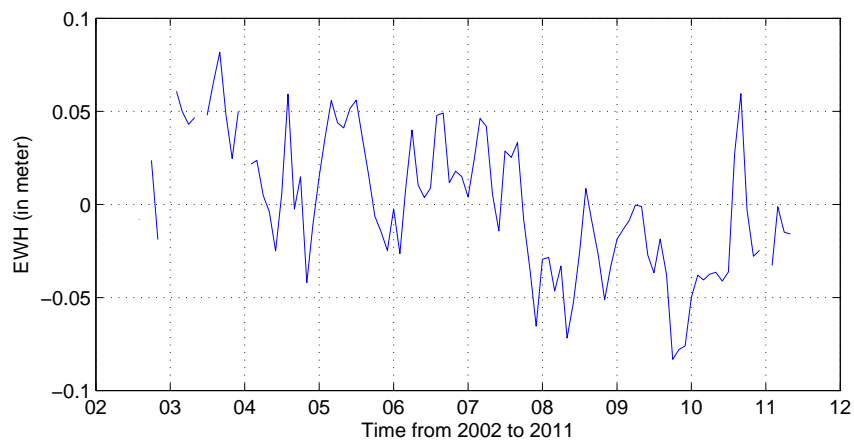
Figure 4.40: Time-series plot of EWH in Indus basin for Pakistan 2010 floods analysis

65

In residuals the signal for flood during 2010 can be seen clearly.
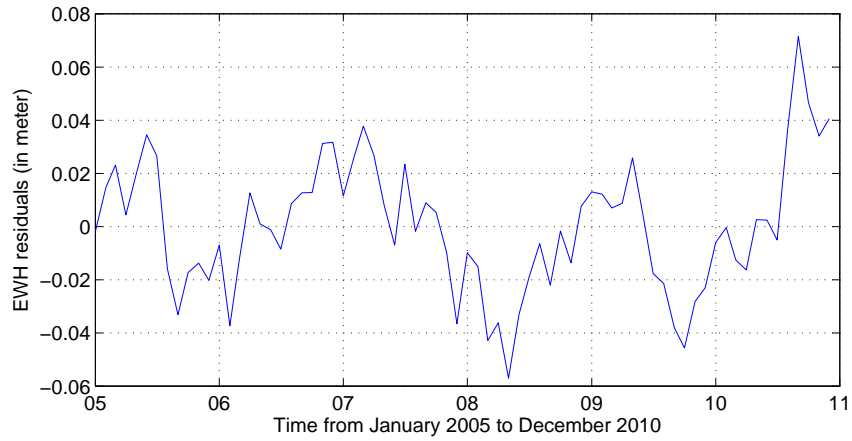
Figure 4.41: Residual plot of EWH in Indus basin for Pakistan 2010 floods analysis

14. Congo river basin: Congo river basin did not experience any floods during the GRACE period rather it went through a regular drought for years, the time series plot discussed in the next section of droughts explains the condition very well.

15. Murray Darling: This south Australian basin covers an area 1,450 km long and 1,000 km wide and consists largely of plains rising to the Great Dividing Range on its eastern and southern rim. This basin is facing drought for the past decade with severe condition in year 2004-2005.

Place	Year	Visible to grace
China	2004	no
Sao Paulo	2004	yes
New Orleans	2005	no
China Fujian	2005	yes
India mumbai	2005	yes
Kenya Ethpoia	2006	yes
North korea	2007	no
African Nation	2007	no
South China	2008	no
India (Bihar)	2008	yes
Taiwan	2009	yes
New Orleans	2009	yes
Amazon basin	2009	yes
Pakistan Indus basin	2010	yes

Table 4.1: Flood event calendar

4.4 Droughts

Droughts are the absence of rain, and thus grow and retreat in severity at rates paced by the climatological (normal) precipitation in an area. Droughts strongly impact agriculture, disrupting the annual harvest cycle, affecting prices for agricultural commodities in real time through market speculation, and through lingering scarcities, rippling through regional and global economies for many months after the drought has ended. In some regions with decadal time scale climate variations, such as the south-western United States or the Sahel in Africa, droughts can persist for many years or even decades.

Droughts are severe when they do not meet annual precipitation on normal scales and the amount of ground water taken out increases continuously. The condition of drought does not only depend on annual rain, in fact when the ground water storage gets depleted either by plant induced capillary effect or by excess consumption by human being along with high temperature taking on high evaporation of soil moisture, accompanied by less annual rainfall, the condition of drought is then announced (West). Droughts are not quick as are floods they take time to happen and take time to retreat. Since lot of water is lost in run-off we cannot assure that heavy rainfall would reduce or finish the condition of drought. Even if we have steady rain, first off all the ground water storage would be replenished in principle, but in how much time, that depends on the nature of the soil. Things cannot be decided at once, but the Condition of drought does have a huge water loss thus, considerable mass change. Droughts occur over large areal extent so we can see pretty good signal on GRACE for droughts. Factors which we need to keep in mind before performing drought analysis are:

1. Drought are fairly visible if we take the whole basin into account since the water nearby river would not change at the rate at which the region away would and when we take a large area the amount of water loss would be large thus a clear signal of hydrological mass loss would show up in time series and residual plot as well.

2. Droughts extending larger than GRACE time period or for major time period of the GRACE life would not show up since when we are looking at either time series or residual plot we look at the deviation from normal behaviour which we consider to be a major part of the GRACE time period. And when we have a continuous drought over the entire GRACE time period we would never see an outlier for drought based on our analysis scheme.

4.4.1 Methodology used and analysis of various basins for droughts

The steps involved in the drought analysis are enumerated below:

1. We prepare a list of all the major droughts throughout the world in the years for which we are analysing the GRACE observed local gravity variations, we also get the duration of a particular drought.

2. For the basin in which the drought was reported, we calculate monthly mean EWH values for whole basin. The mean for every month is represented in the time-series as individual points. Then we generate the residual plot for the same area by following the methodology discussed in the section residual plot.

3. Observe the time-series, if the drought occurred in the dry season then since every year we get the water level decay in the region in that part of year, the annual GRACE cycle would be giving a low every time in that part of year. So, we would get a distinguished low value of EWH for few months due to a drought reported, among usual low for the same months of rest of the years. If the drought occurred in the rainy season or any season other than dry then searching low value points in the time-series is not a good idea rather the elevation in annual cycle observed every year would appear less elevated for the month or time frame in which the drought is reported. In the case discussed later residuals are very helpful since they describe the anomalous behaviour from the mean behaviour and droughts would always appear to be a low.

   The precipitation plots cannot be trusted blindly since a heavy rain for a short duration might not be able to pull the area from drought. Also for the other case, even sometimes precipitation might be normal throughout the year but not sufficient to refill the groundwater storage (due to high rate of groundwater usage or heat waves making lot of water to evaporate) and account for high evaporation of water contained in soil moisture due to extremely hot weather. We must be careful before saying firmly whether this particular drought might be seen by GRACE alone or along with precipitation and run-off data as well. We will start the drought analysis with the major river basins.Amazon basin

   Amazon gives the largest GRACE signal and is well known for its hydrological signal. It experienced two major droughts in the last decade on in the year 2005 and other in

2010. Both these are visible clearly in GRACE. (Back in October, Brazil declared a state of emergency in the state of Amazonas due to record low water levels. After that, little rain had fallen and the situation got even worsened. According to The New York Times, the Brazilian Armed Forces have mounted the largest relief operation in their history, delivering some 2,000 tons of food and 30 tons of medicine to affected communities just in the region (Butler [2005]).) Amazon rainfall in 2005 was indeed below normal, but the deficit was not particularly large. Rather, it was the last episode of an unusually long drought started in 2002, leading to the severe depletion of soil moisture and lowering of water levels. The whole Amazon basin was considered for Drought analysis and we can see exceptional low value of EWH in time-series (Figure 4.42) itself which gets more pronounced on residual plot (Figure 4.43) against years 2005 and 2010.
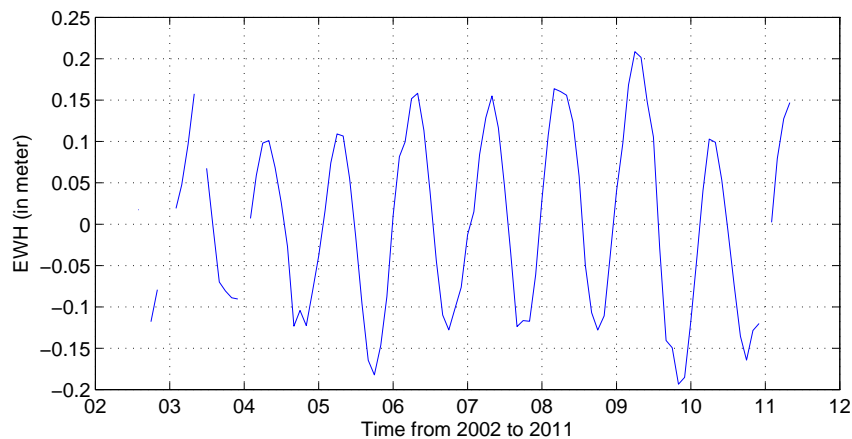
Figure 4.42: Time-series plot of EWH for Amazon 2005, 2010 drought analysis

1. In residuals the signal for droughts during 2005 and 2010 can be seen clearly.
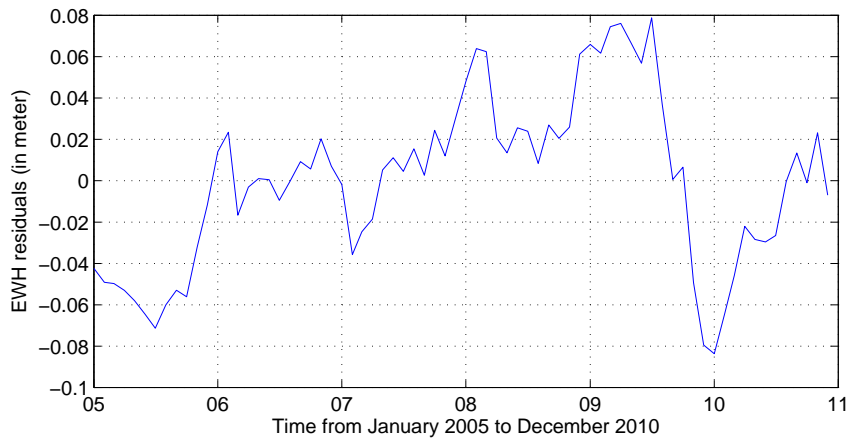
Figure 4.43: Residual plot for Amazon 2005, 2010 drought analysis

2. Congo river basin

   It is the second largest river basin and also gives a strong signal. But it has been
   through a period of drought for the last decade, only in later part of the year 2007 the
   precipitation conditions were good enough to pull it out from drought. We can see the
   drought in the residual plot in the few initial years of the GRACE time period, especially
   2006.

71
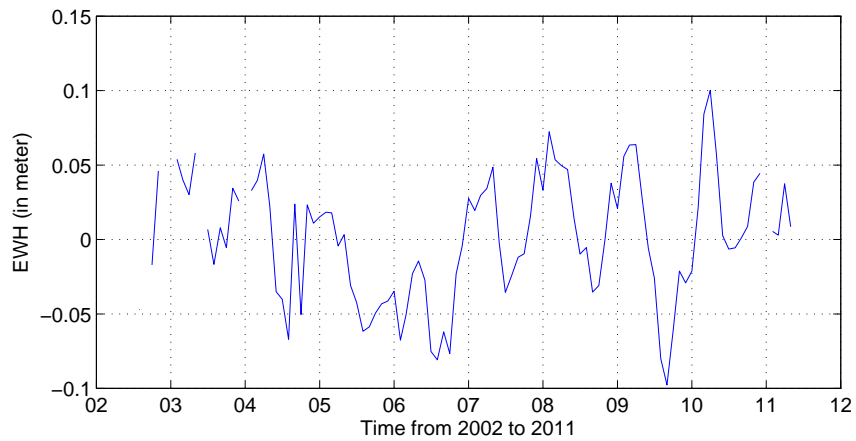
Figure 4.44: Time-series plot of EWH for Congo basin drought analysis

In residuals the signal for droughts (low value of EWH) during 2006 as well as 2009 can be seen clearly.
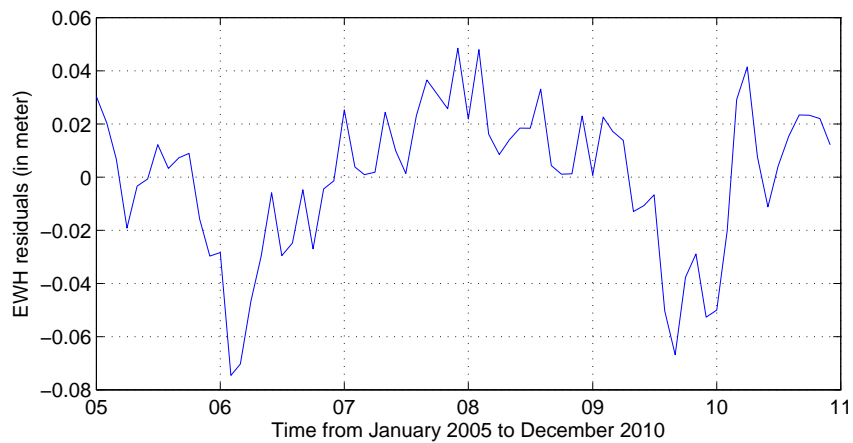
Figure 4.45: Residual plot for Congo basin drought analysis

3. Mississippi river drought

   The Mississippi river experienced drought from 2006 to 2007 and came out of drought condition in 2008. It can be seen in the time-series and residual plot as well.
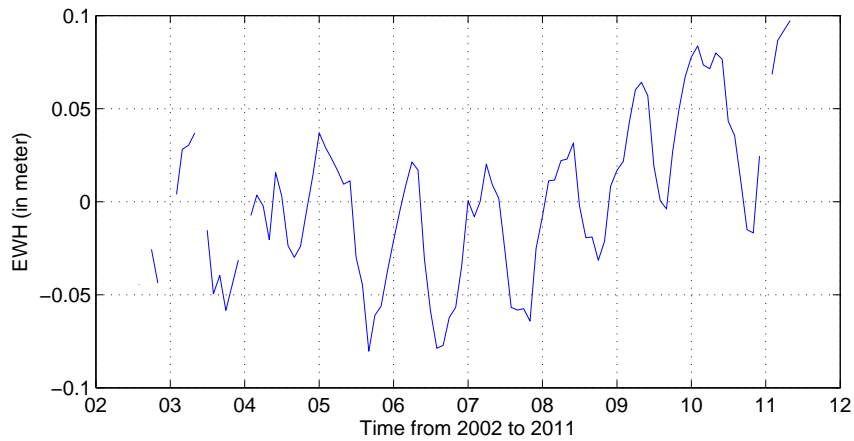
Figure 4.46: Time-series plot of EWH for Mississippi river drought analysis

In residuals the signal for droughts (low value of EWH) during 2006 and 2007 can be seen clearly.
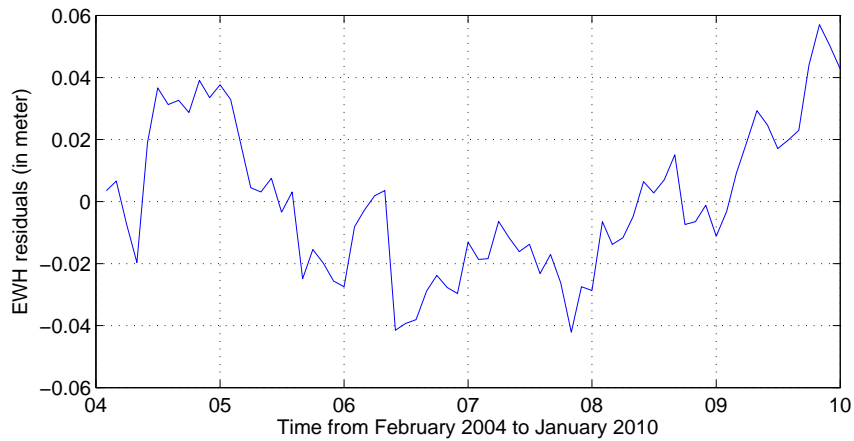
Figure 4.47: Residual plot for Mississippi river drought analysis

4. Murray darling river basin drought

   Murray darling river basin has been in a state of drought for a long time in the previous decade (marc J. Leblanc [2009]). it experienced worst drought in the last decade in the

years 2006 and 2007 followed by recovery at the end of 2007, however the drought came again in the years 2008 and 2009 but not so intense as it was in 2006 and 2007. These facts can be observed in the residual plot for the basin very well.
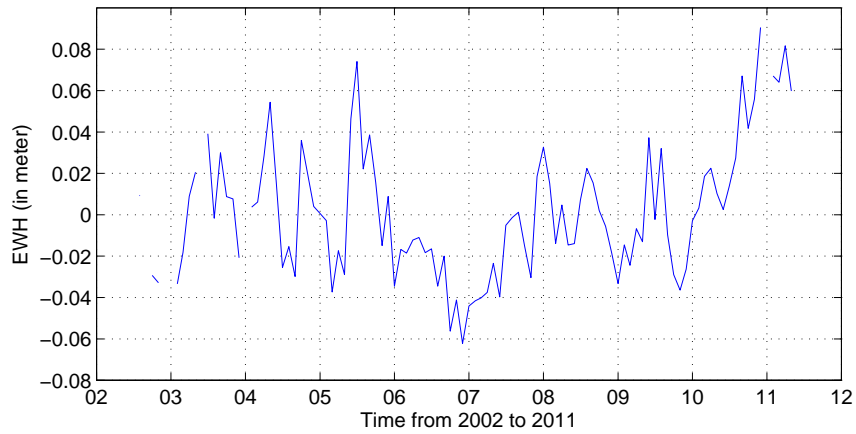
Figure 4.48: Time-series plot of EWH for Murray Darling river basin drought analysis

In the residuals, the signal for droughts during 2006 and 2007 can be seen clearly. The time-series for the years 2008 and 2009 show small positive peaks for few months but mostly the residuals are negative, and the reason is that since for most of the GRACE observed time there was dry condition, 2006 and 2007 being most dry and 2008 and 2009 being less dry.
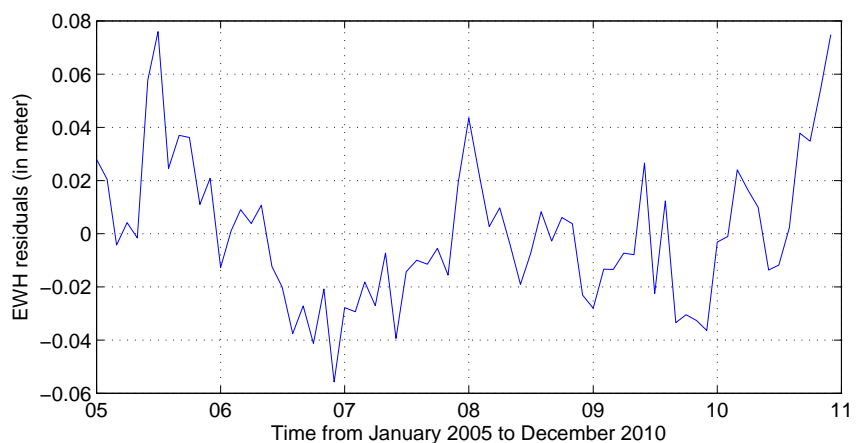
Figure 4.49: Residual plot for Murray Darling river basin drought analysis

74

5. Nile river basin

Nile river basin in the African continent has been under a long decade of drought vis-
a-vis Congo, since most of the GRACE observations were made during this period of
drought so the mean or normal behaviour reflected is that of dry conditions. Thus we
get only 2009 and 2006 as the lowest point out of which only 2009 can be said to be
drought by looking at residual plot. In this case time-series serves a better purpose and
shows that only 2007 and 2008 show no sign of drought; higher values of EWH and rest
of the years have lesser EWH value.
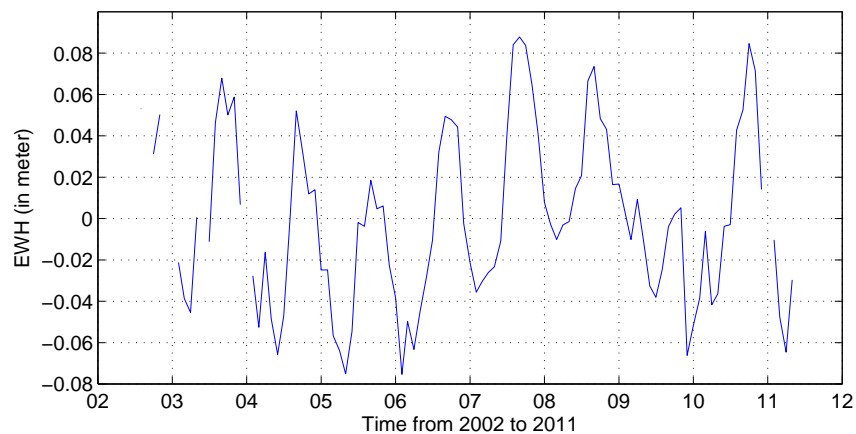
Figure 4.50: Time-series plot for Nile river basin drought analysis

In residuals the signal for droughts (low value of EWH) during 2006 and 2009 can be
seen clearly.
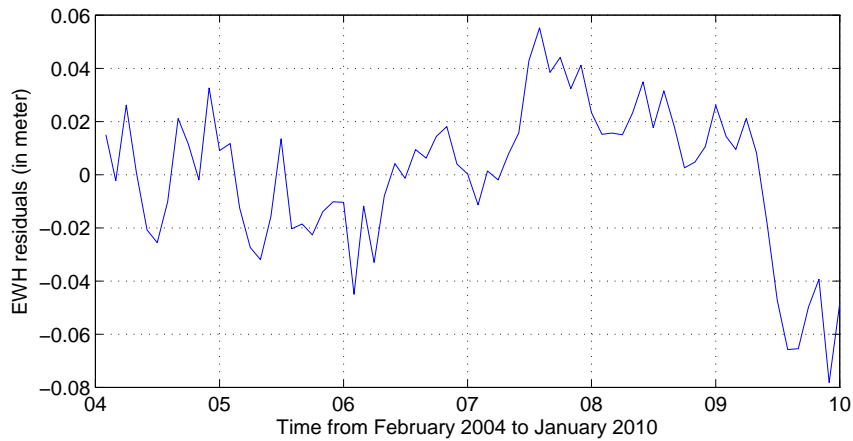
Figure 4.51: Residual plot for Nile river basin drought analysis

6. Yangtze river basin drought

This Chinese river basin experienced a severe drought session from 2006 to 2007 and then after good rainfall in 2008 it again experienced dry season in year 2009 and 2010. These observations are very clearly visible in Time-series and residual plots. Time-series plot shows 2006-2007 drought clearly while the 2009-2010 condition can only be assessed by looking at residual plot.
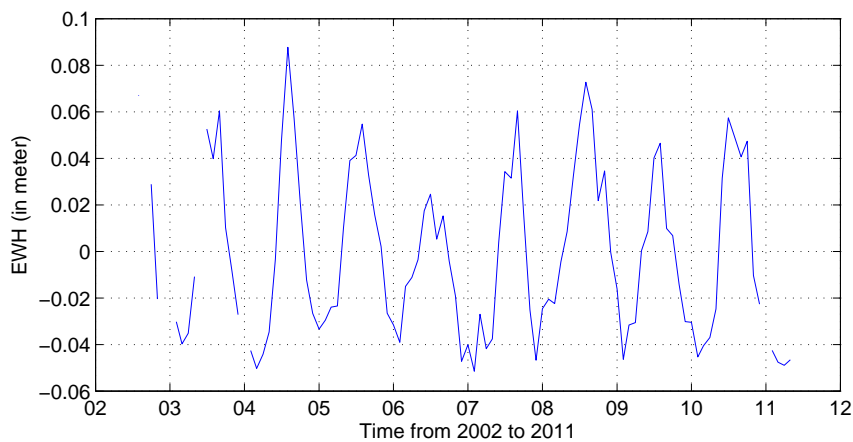
Figure 4.52: Time-series plot for Yangtze river drought analysis

In residuals the signal for droughts during 2006, 2007, 2009 and 2010 can be seen clearly.

76
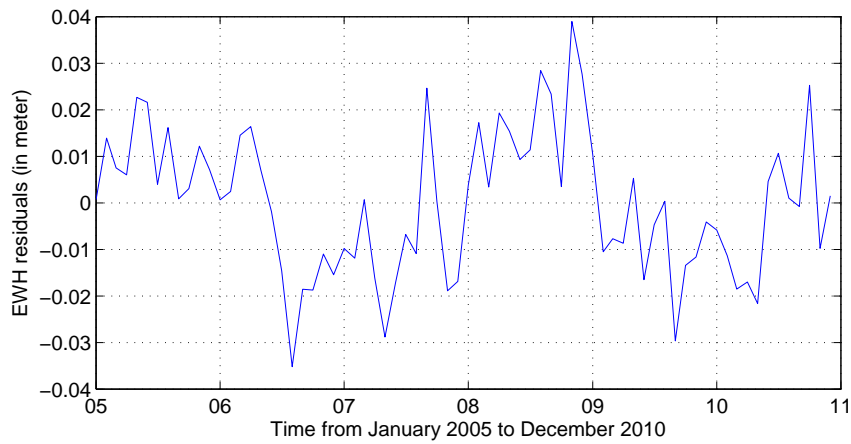
Figure 4.53: Residual plot for Yangtze river drought analysis

7. Colorado drought 2008 and 2009

United states provinces along Colorado river experienced extreme dry year as per usgs report. The river basin drying out due to climate is suspected to bring severe drought. We are not able to observe dry year of 2009 in the time-series plot and neither in residual plot. The 2008 drying is visible but only in residual plot.

Place	Years	Visible to grace
Amazon river basin	2005, 2010	yes
Congo river basin	2000 to 2007	yes
Mississippi river basin	2006 to 2007	yes
Nile river basin	2000 to 2007	no
Murray river basin	2006 to 2009	yes
Yangtze river basin	2006	yes
Colorado drought	2008,2009	no(2009),yes(2008)

Table 4.2: Drought event calendar

Chapter 5

Earthquakes and rising volcanoes

5.1 Introduction

Tectonic activities have been changing the shape of earth for millions of years. The earth is made up of different type of materials which behave in numerous ways when subjected to stress. So we get different types of landforms at different places and also the nature of stress applied is an important factor in deciding the type of change. Continental crust has been going through slow continuous, and sudden changes (occurring in episodes)as well since the Earth has existed. We have two different categories for these changes, crustal formation processes and crustal deformation processes.

Crustal formation processes are driven by our planets internal energy, and the exogenic processes of weathering and erosion, powered by Sun. These activities are slow, taking millions of years and they result in gradual uplift and new landforms such as mountain-building. The main three types of landforms we witness due to these processes are:

1. Residual mountains and continental cores, example: Canadian shield, Alaska, British Colombia, and mountain west.

2. Tectonic mountains and landforms, example: Himalayas, Wrangallia, Cache Creek.

3. Volcanic features, example: Bolivia.

Crustal deformation processes are seen when any type of surface (made of any type of rock) is subjected to stress by tectonic forces, gravity, and the weight of overlying rocks. The types of stress which can be observed are tension, compression and shear. The result of stress

is strain which can be either folding or faulting. The strain observed depends on property of material of the surface (brittle or ductile), the pressure the surface (rock) experiences and the direction of force. The strain observed may be classified as normal fault, reverse fault and strike slip fault in terms of faulting. The next figure show these faulting and their related stresses.
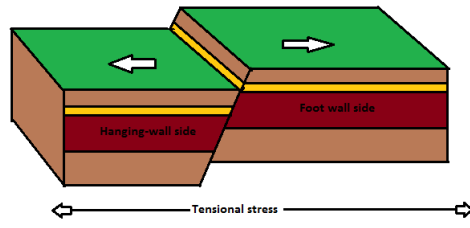
(a) Normal faulting
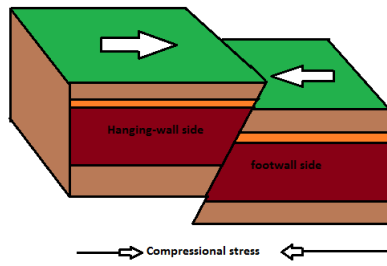
(b) Thrust reverse faulting
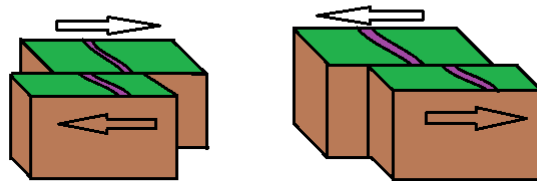
(c) Strike-slip faulting

Figure 5.1: Types of faults

When any of these faulting occurs, the rocks on either side are displaced relatively and at the time of fracture a sharp release of energy occurs which is called *earthquake*. The crustal plates do not move smoothly along, rather there is a lot of friction along plate boundary so when stress due to relative motion becomes more than the frictional force then a sudden motion occurs, releasing enormous seismic energy. This energy is experienced around the globe but the magnitude is very small away from epicentre, so we can feel earthquakes when we are close to the epicentre. There are many observatories recording the waves generated round the globe to study the Earth's interior composition. These waves generated are low frequency waves. The earthquakes are recorded on Richter Magnitude Scale, which refers to a number of ways to assign a single number to represent the energy contained in an earthquake. In all cases, the magnitude is a base-10 logarithmic scale obtained by calculating the logarithm of the amplitude of waves measured by a seismograph. Moment magnitude scale is now used to denote the energy released in an earthquake. It is denoted by M_w, and it is dimensionless (KANAMORI and ANDERSON [1975]). The relation between magnitude of seismic moment (M_0) and moment magnitude (M_w) is:

$$M_w = \frac{2}{3}(\log_{10} M_0 - 6.07) \tag{5.1}$$

5.2 Earthquake as seen by grace

Earthquakes do produce mass redistribution and if they are of a particular fault type and with enough energy their affect can be observed by GRACE. There are several other effects which are very much pronounced and they are reflected in the spherical harmonic coefficients describing the Earths potential field variations over time. The earthquakes change the Earth oblateness which can be observed by changes in J_2 that is ΔC_{20}. They make the rotational pole drift toward ≈ 150 degree east. These affects are analysed by normal mode theory for major earthquakes in the time frame of 1977-85 by B. Fong Chao [1987]. Normal mode theory is used to study oscillations due to disturbance by earthquake on earth. The seismic waves travel over the surface of earth in each direction after earthquake. These waves would meet at the diametrically opposite end of the sphere if the earth is assumed to be homogeneous and perfect figure. Then these would interfere amongst each other to provide interference pattern, which could be additive, subtractive, or even standing waves depending upon what

type of geological feature a wave has to cross. The fundamental frequency and its overtones can be further studied to define properties of Earth. The frequency spectrum analysis can reveal a lot about the processes. Tidal deformations have line spectra at fixed frequencies. Meteorological variations in atmosphere and hydrosphere have seasonal and high frequency components. Slow and continuous processes such as deglaciation, and other crust formation processes have red spectrum and varies as f^{-4}, where f is frequency. The seismicity have a spectral dependence of f^{-2} and is random and they effect the rotation of earth in order to conserve angular momentum (B. Fong Chao [1987]). Earthquakes are negligible in changing Earth rotation. The normal modes pointed out for earthquakes are spheroidal and toroidal. Toroidal modes generate no density change; only the spheroidal modes are useful to study density changes. The density changes are observed as changes in total moment of inertia of the Earth. Chao and Gross demonstrated that the ΔC_{20} shows significant change and non randomness as compared to ΔC_{30}, ΔC_{40} and ΔC_{50}. ΔC_{20} showed a trend of decrease thus conclusion was drawn that the earthquakes tend to make earth more spherical and reduce oblateness.

A gravity mission similar to GRACE, with inter-satellite ranging and low orbit at 160 km was proposed in 1986 to detect rebound from ancient de-glaciation, very large dip-slip earthquakes, detailed ocean tides, and seasonal growth and decay of continental glacial fields. It was named Geopotential Research Mission (GRM). They gave a proper insight to what limit can we use such mission to observe gravity changes made by an earthquake (Carl A. Wagner [1986]). They showed that the amplitude A of the range rate signal for great earthquake is roughly proportional to the fault area. The precision measurement (for range rate) for GRM mission was 1 micrometer per second. GRACE has inter-satellite range rate signal amplitude of 2 micrometer per second so, the relation gave the value of detectable earthquake by GRM mission to have a magnitude moment of 8.36. The relation used is given below

$$A = X_1 \left(M/X_0 \right)^{2/3} \tag{5.2}$$

where X_1 and X_0 are constant having value 15 micron per sec and 8×10^{29} dyn cm respectively. M is the moment magnitude of detectable earthquake.

Similarly for GRACE mission we can calculate the range of earthquake magnitude moment which can be seen. GRACE has a range rate amplitude of 2 micrometer per second, we get

the corresponding magnitude moment of detectable earthquake to be 8.36. Thus all the earthquake of magnitude less than 8.36 are not visible in GRACE time-series ideally. But there are errors in GRACE measurements so the limiting value must be a more higher, well after carrying out time-series analysis in this thesis work we observed that there are many other factors which should be considered to decide whether we would be able to see a earthquake or not.

Few earthquakes in the time slot of 2002 to 2011 are analysed by various people, mainly the Sumatran earthquake of December 2004. The level 2 data is not that efficient for earthquake analysis unless the magnitude is too large. The level 1-B data is most preferred by people. The work by Shin-Chan Han [2006] on Sumatra Andaman earthquake gives a good view to what we can expect from GRACE. While studying for the 9.3 magnitude Sumatra-Andaman earthquake which ruptured more than 1000 km of a locked subduction interface, they used the KBR-SST data along with accelerometer and attitude data. He enhanced the temporal and spatial resolution for better field variation observations. They compared the results with predicted gravity changes from seismically derived dislocation model to infer that GRACE observations are in excellent agreement. The power spectrum of gravity changes induced by dilation from the seismic model suggests that the most power are at low degrees. The SNR at high degree is poor; most of the signals are within less than 40 to 50 degrees. GRACE would miss the main power of the uplift and subsidence but it successfully captures the main power of dilatation.GRACE retains only 2% of the power of uplift and subsidence signals while 50% of the power of dilatation signals. Thus strike-slip faults are showed extremely well by GRACE while other types of faults will not show up significantly.

Shin chan han et. al., also investigated the Maule (Chile) magnitude 8.8 earthquake for the regional gravity decrease. He observed a gravity anomaly of about -15 microGal around the epicenter (Shin-Chan Han [2010]). For this study the data used was satellite to satellite tracking data. The results were in agreement with the gravity change predicted from the finite fault models.

We used the release-04 level 02 data set only. The parameter for observation chosen by us is geoid height instead of gravity anomaly as the gravity is gradient of potential so the geoid height curves are smoother and thus randomness is less. The interpretation by looking at plots for geoid height is much more beneficial than at those looking at gravity anomaly. The methodology which we implemented consist of taking three points, one at epicentre and

the other two at the two different plates due to whose interaction the earthquake occurred. These pixels are taken 5 degree away from epicentre thus, spatially they are at a distance of $\approx$ 555 km from epicentre on two different plates. The time-series are generated for these three points and drawn on same plot. Then on observing the three curves we can see a sudden change in the geoid value along with the reversal of relative position of time-series of the two points on different plates. One observation is that for every earthquake assessment there was a dip in the time-series in the end of 2009. This is due to anomalously large variability in ΔC_{20}. The ΔC_{20} coefficient is the largest signal in GRACE data set and it accounts for the Earths oblateness thus it is the major coefficient describing geoid and its instability makes geoid poor. The large variability of this coefficient is illustrated in the figure 5.2, there is comparison between the Satellite Laser Ranging (SLR) generated ΔC_{20}.
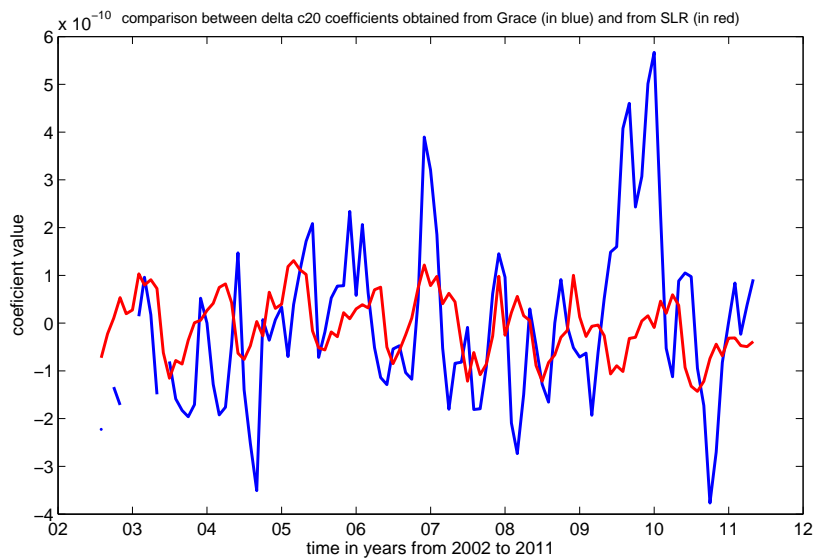
Figure 5.2: Comparison between ΔC_{20} obtained from GRACE and that from SLR

The plot shows that GRACE ΔC_{20} is very infidel during start of 2007 and even more worse during 2009. Thus for better interpretation we replaced ΔC_{20} from GRACE by ΔC_{20} obtained from SLR to get rid of the erroneous dip at end of 2009. This replacement showed improvement in the geoid plots.

5.2.1 Methodology used

We took three points, one at epicentre and other two at two tectonic plates interacting with each other. To take into account the limitations of GRACE spatial resolution data we took the two points on different plates 5 degree away from epicentre. The basic idea is to study the changes in the geoid height anomaly of plates before and after earthquake. The two plates interacting experience substantial amount of change before and after earthquake, and also with respect to each other. Our aim is to see this change and analyse them according to the nature of earthquake and its intensity. The relative change between plates would allow us to comment on type of fault, and the change before and after the earthquake would help us to comment on its visibility to GRACE. We will now discuss the effect of earthquakes on GRACE observed time series of geoid heights in the next section.

The major earthquakes with magnitude greater than 8.36 which occurred in the last decade are discussed below:

1. Sumatra Andaman December 2004 9.3 Mw earthquake

   The geoid plot shows a variation from +5.8 mm to -4.8 mm. The time-series for point on Eurasian plate denoted by red initially is having higher geoid height than the indo-Australian plate till the occurrence of earthquake on December 2004. After that there is a sudden dip in the geoid value of all the three points and their geoid height do not show large differences as they showed before the occurrence of earthquake. Rather, when we observe the time-series for the time onwards the earthquake occurrence they switch their positions. This earthquake activity was strike slip and we observe the three curves at three points to be in phase suggesting that the nature of activity was not thrust reverse fault, neither normal faulting but strike-slip. First of all we would look at the time-series generated by GRACE data alone without replacing ΔC_{20} then we would look at the time-series plot with replaced ΔC_{20}. We can notice the improvement in geoid height value in the time-series at the end of year 2009.
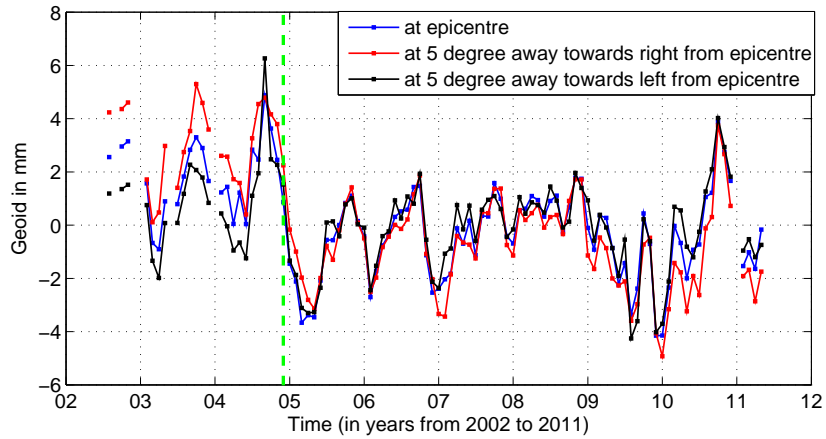
Figure 5.3: Time-series plot of geoid heights for Andaman-Sumatra earthquake analysis with GRACE ΔC_{20}
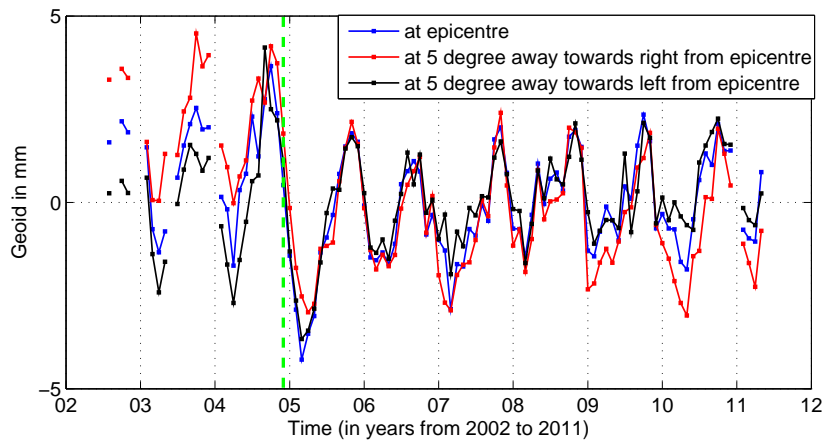
Figure 5.4: Time-series plot of geoid heights for Andaman-Sumatra earthquake analysis with replaced ΔC_{20}

2. Chile February 2010 8.8 Mw earthquake

The variation of geoid height for the south American plate shows a good annual cycle

87

thus some hydrology is involved while the other point on Nazca plate is not showing any such behaviour of strong seasonal signal. At the point of occurrence of earthquake a steep dip is observable. This event was normal faulting event, and we observe that the two plates are in phase but out of phase with the epicentre. We interchanged the ΔC_{20} coefficients of GRACE with that from SLR so the results are not dubious. Although the accuracy of results is not good since after 2009 end GRACE performance has not been good enough. We would look into first the pure GRACE data and then next with replaced ΔC_{20}.
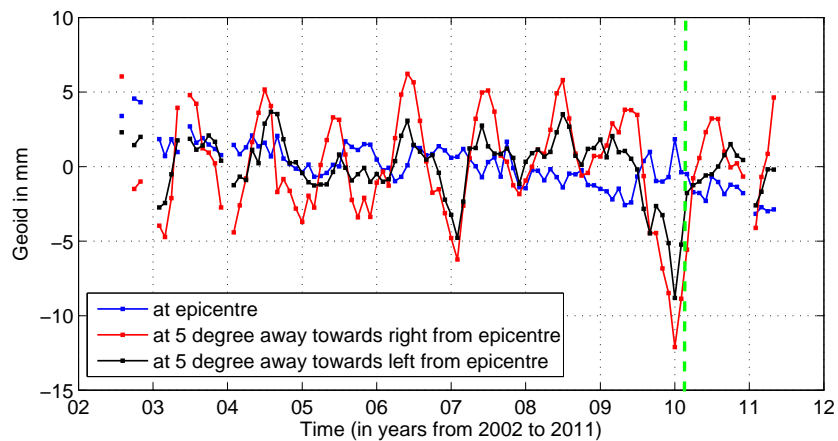
Figure 5.5: Time-series plot of geoid heights for Chile earthquake analysis with GRACE ΔC_{20}
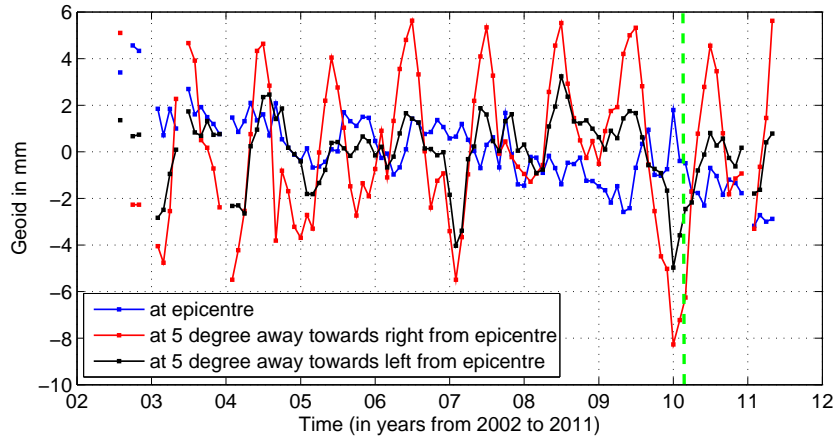
Figure 5.6: Time-series plot of geoid heights for Chile analysis with replaced ΔC_{20}

Place	Magnitude	Time	Visible to grace
Sumatra Andaman	9.3	Dec 2004	yes
Northern Sumatra	8.7	Mar 2005	no
Sumatra Indonesia	8.5	Sep 2007	no
Chile	8.8	Feb 2010	yes

Table 5.1: Earthquake event calendar

5.3 Volcanoes seen by grace

Volcanic activities are a part of crustal formation processes, which our earth is undergoing from time to time. There are more than 1300 volcanoes identified and less around 600 of them are active. In an average year about 50 volcanoes erupt worldwide. A volcano forms at the end of a central vent or pipe that rises the asthenosphere and upper mantle below through the crust into a volcanic mountain. A crater or circular surface depression usually forms at or near the summit. Magma rises and gets collected near the surface until conditions are not approached. This upward thrust makes the surface to bulge out and thus we observe mass redistribution.

Nearly all of the volcanic areas are small on spatial scale, thus we cannot see them by GRACE unless the mass redistribution is enormous. Two largest bulging volcanoes are investigated in this thesis, which were reported to be bulging very rapidly and also the area is larger than any other volcano. The spatial extent is not of GRACE spatial scale. The motivation with which we tried to analyse their rise with time is that, they might be small but the mass redistributed each year is not small and we might get a small signal although not as strong as it appears to be theoretically but averaged value of it over GRACE spatial scale. This reduced signal is due to the fact that the mass redistributed per unit area at the place of activity is more but when we take the GRACE spatial scale of 400 km we have to take the mass redistributed over an area of volcano per 400 km. The two volcanoes studied are those located at Yellowstone, Caldera, North America and at Uturuncu, Bolivia,South America. These two volcanoes have been reported to be inflating at a very rapid rate. According to science observation team Caldera super volcano Yellowstone is North America's largest volcanic field, produced by a "hotspot" a gigantic plume of hot and molten rock that begins at least 644 km beneath Earth's surface and rises to 48 km underground, where it widens to about 482 km across. There, blobs of magma or molten rock occasionally break off from the top of the plume, and rise farther, resupplying the magma chamber beneath the Yellowstone caldera. Scientists from University of Utah reported that the Yellowstone super volcano rose at a record rate since mid-2004, likely because a Los Angeles-sized, pancake-shaped blob of molten rock was injected 6 miles beneath the slumbering giant. The upward movement of the Yellowstone Caldera floor was recorded to be 3 inches or approximately 7 cm per year for the from 2004 and is more than three times greater than ever observed since such measurements

began in 1923. Previous research indicated that the magma chamber began about 5 miles beneath Yellowstone and extends down to a depth of at least 10 miles. Its heat powers Yellowstone's geysers and hot springs the world's largest hydrothermal field. Thus the amount of mass moving up is enormous and this thought motivated us to look at this volcano by GRACE.

The North American super volcano shows a good annual seasonal cycle, which is due to hydrology involved since there are geysers and lake. The South American super volcano cannot be seen in GRACE. We used the GRACE geoid height with the replaced ΔC_{20} coefficient from SLR. We observed a gradual increase in the mass as the annual cycles seems to be following a positive trend for North American super volcano. The slope of trend was calculated to be 0.052 mm per year. The time-series and trend are shown in figure 5.7 and 5.8 respectively.
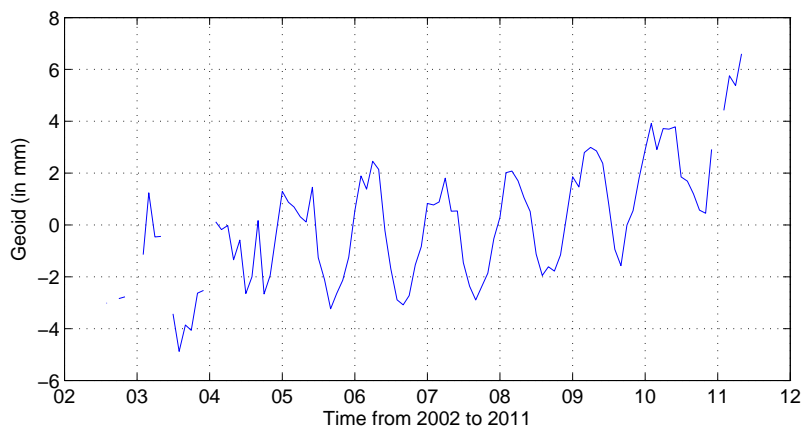
Figure 5.7: Time-series plot for Caldera Yellowstone super-volcano analysis

91
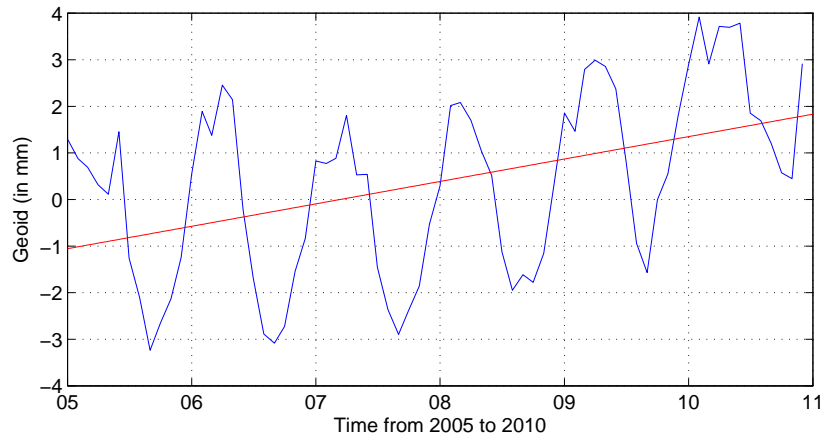
Figure 5.8: Trend estimation for Caldera Yellowstone super-volcano

The South American super volcano was reported to be rising in October 2011; the data set of GRACE We are working with has monthly gravity solutions only till may 2011. The gravity solutions after 2010 are not so good because GRACE had several problems since 2011. We tried to plot the time series for this volcano also. There were no observations sufficient to illustrate the rising volcano in GRACE, the possible explanations are; the area is not that large to show changes properly, also that the major changes took place in 2011 while we are working with data up to may 2011 only and trend analysis would not show changes due to activity in last few months when there is no activity for rest of data. The signal must be weak and that would become even weaker on a spatial scale of 400 km. The time-series and trend estimate plot are shown in figure 5.9 and 5.10. The trend observed was negative and it might be due to loss of soil moisture at high rate due to heated surface created by volcanic activity in the region.
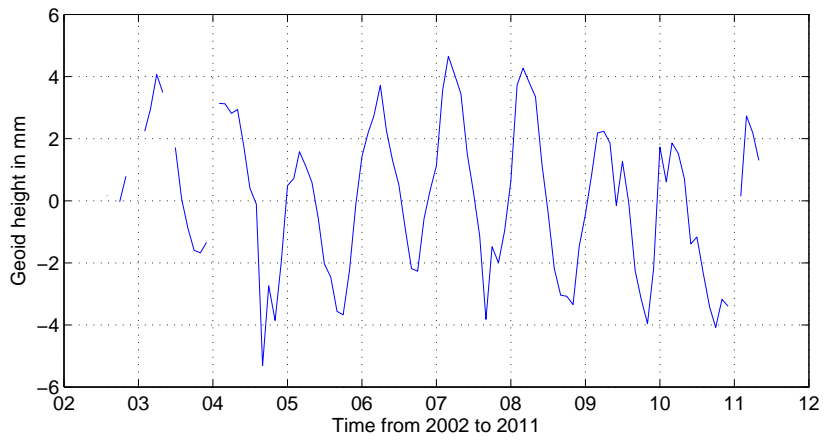
Figure 5.9: Time-series plot for Bolivia super-volcano analysis
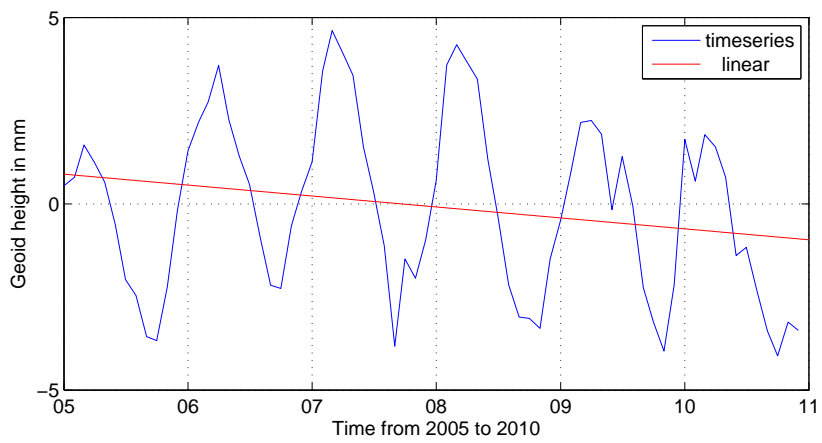
Figure 5.10: Trend estimation for Bolivia super-volcano

93

Chapter 6

Trends in Glacier and ice cap mass

6.1 Introduction

The world's ice sheets, ice caps and glaciers are important indicators of global warming. Their retreat and higher rate of melting has contributed maximum to the increasing concern over alarming rate of global sea level rise. Three main contributors are ice sheets, ice caps and mountain glaciers. Amongst them mountain glaciers and ice caps contribute more than ice sheets to global sea level rise. This mass reduction in glaciers of large spatial extent can be read by GRACE. There is now clear evidence that the retreat of glaciers in many locations of the world has accelerated in recent decades. Glacier retreat provides a clear indication of a global climate that has been warming since the Little Ice Age (LIA), which occurred from approximately 1650 to 1850. The glaciers at a height of 4000 m to 7000 m have not responded to the global warming but the glaciers at lower heights are recorded to show retreat. The simplest method to observe whether glaciers are affected by the global warming is to record the annual terminus of glacier. This method is not accurate since the change in mass at greater heights is not taken into account.

There has been already a lot of work on glaciers with GRACE data and these studies show that GRACE is a potential instrument to study glacier mass changes. For Greenland ice cap chen et al compared the results derived from GRACE and those from satellite radar interferometry data for the time period from April 2002 to November 2005. The estimation of total ice melting rate from GRACE was calculated to be -239 $\pm$ 23 km^3 / year and the estimate from satellite radar interferometry was -224 $\pm$ 41 km^3. so the results are in good agreement. Baur et. al., pointed out that along with quantification of ice mass loss from ice cap of Greenland

we should have the spatial localization of these losses also. He used technique of point mass modeling to derive mass-balance patterns from GRACE gravimetry in the south-east coastal region of Greenland (Oliver Baur [2011]). Chen et. al., also investigated about glacial melting in Alaskan mountain. He separated the local groundwater changes from the GRACE observations to get the glacial mass change. The terrestrial water storage estimates were derived from an advanced land surface model. The glacial melting observed by GRACE is equivalent to -101 $\pm$ 22 cubic km per year, which is in agreement with airborne laser altimetry data estimate of -96 $\pm$ 356 cubic km per year (J. L. Chen [2006]). Luthcke et. al., also investigated for Gulf of Alaska region, he used mascon solutions for GRACE estimated gravity variations. He estimated the total mass balance loss to be -84 $\pm$ 5 Pg/year. His results were in agreement with aircraft altimetry and in-situ measurements (Scott b. Luthcke [2008]). These glaciers and ice caps discussed are in the very north of northern hemisphere while we also have a study done by Immerzeel et. al., on Asian glaciers feeding Ganges and Brahmaputra, his trends estimated a negative trend of 0.22 $\pm$ 0.05 m/year in the Ganges basin (Walter W. Immerzeel [2010]).

The work done by different people for different area suggest that the fast receding glaciers are reflected in the GRACE data set.

6.2   Analysis of few glaciers

1. Greenland ice-cap melting

To start with, first we would analyse the trend for EWH variations in Greenland. We selected a region in south-east Greenland for analysis. The area selected is shown in figure 6.1.

Figure 6.1: Selected region in Greenland for trend analysis of EWH

The time-series plot in figure 6.2 for Greenland region shows a constant decline.

Figure 6.2: Time-series plot for Greenland region

The trend calculation needs integer number of years so we considered time from 2005 to 2010. The trend was calculated to be 13.14 mm of EWH per year. The figure 6.3 shows the trend.
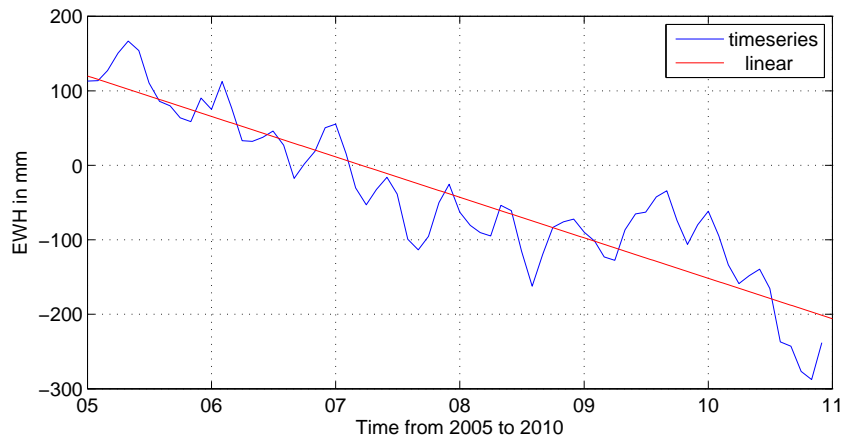
Figure 6.3: Trend plot for Greenland region

2. Gangotri and nearby glacier analysis Gangotri glacier is one of the fastest receding glaciers. The area covered by this glacier is very small for GRACE spatial resolution, so we took a 4 degree × 4 degree grid which includes Gangotri glacier and nearby small glaciers and ice sheets. We observe a negative trend advocating the research results conveying fast melting of glaciers. But GRACE observes whole mass changes so we can not remove groundwater storage changes from data without in-situ data. The area selected, time-series and trend are shown in figure 6.4, 6.5, and 6.6 respectively.

Figure 6.4: Selected region for trend analysis of EWH changes in Gangotri, India

The time-series plot in the next figure for Greenland region shows a constant decline.
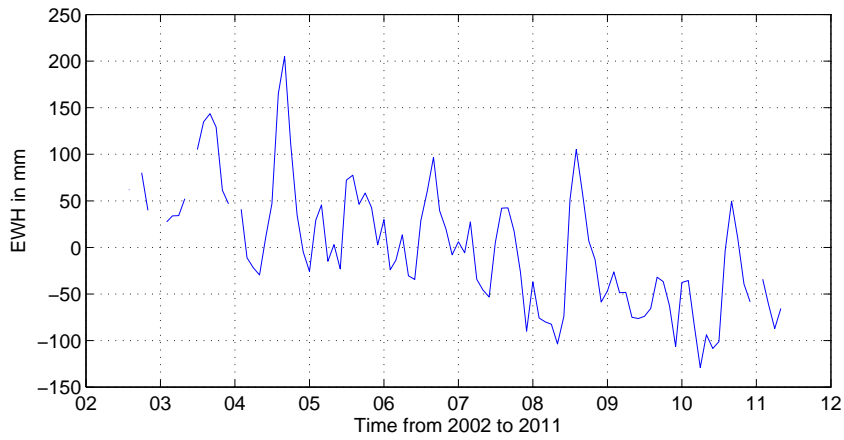
Figure 6.5: Time-series plot for Gangotri region

The trend calculation needs integer number of years so we considered time from 2005 to 2010. The trend was calculated to be 16.54 mm of EWH per year.
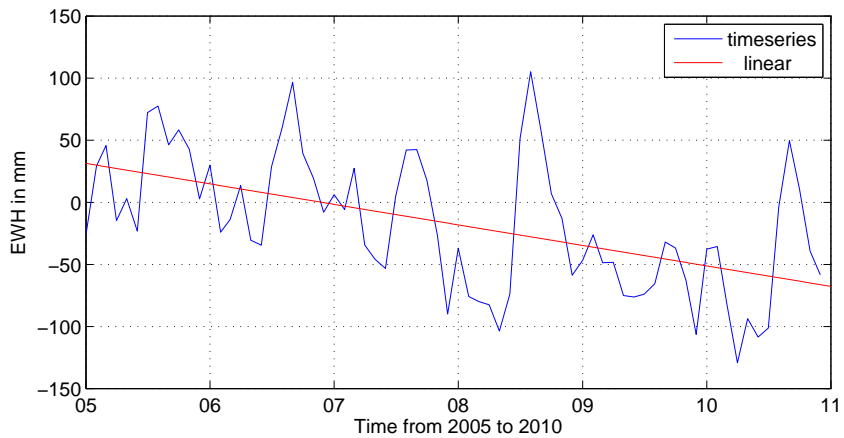
Figure 6.6: Trend plot for Gangotri region

3. Siachin and nearby glacier analysis Siachin glacier is the longest glacier and they also have been reported to be melting at very high rates in the last decade. The GRACE observed mass changes in this region also suggested that they have been receding at

99

very fast rate. The major consideration in this work was that the area covered by glacier was small for GRACE spatial resolution so we again selected a 4 degree × 4 degree area for analysis, encompassing nearby glaciers also. The selected area, time-series and trend are shown in figure 6.7, 6.8 and 6.9 respectively.

Figure 6.7: Selected region in Siachin, India for trend analysis of EWH

The time-series plot in the next figure for Siachin region shows a constant declination.
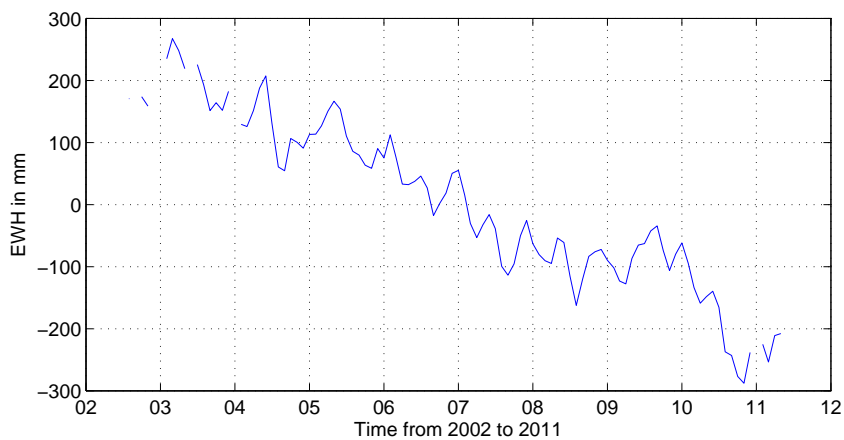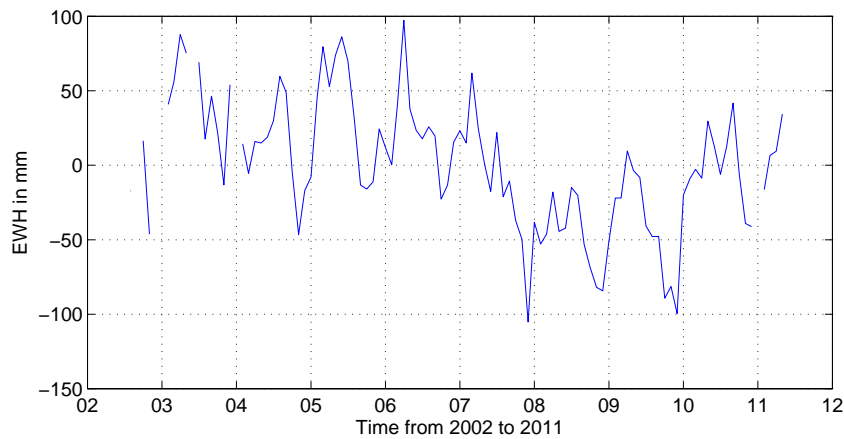

Figure 6.8: Time-series plot for Siachin region

The trend calculation needs integer number of years so we considered time from 2005

to 2010. The trend was calculated to be 13.14 mm of ᴇᴡʜ per year.
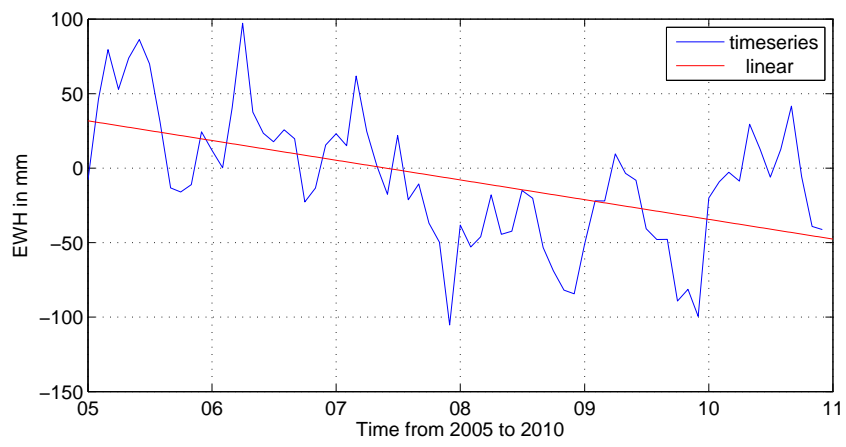
Figure 6.9: Trend plot for Siachin region

Chapter 7

Conclusions and outlook

GRACE mission is of utmost importance for climate sciences and earth sciences studies. The spatial resolution of GRACE is a major limitation while analysing many natural phenomenon. The dependence of spatial resolution on the degree and order of the spherical harmonic terms used, and variation of errors with degree and order made it very clear that events at spatial scale of less than 400 km are difficult to be seen by GRACE unless they produce a strong effect. The major hydrological activities such as floods and droughts, seismic events such as earthquake and volcanoes were discussed to frame a methodology for observing the mass redistribution produced by them. Glaciers were also analysed and the trend suggested their mass decline. The conclusions and recommendations for these fields are discussed in their respective sections below.

7.1 Hydrology

7.1.1 Conclusions

The initial work done was mostly related to the change in terrestrial water storage changes and basin modelling in the field of hydrology. Floods and droughts were observed in this thesis work. These activities were not visible until and unless we would follow some specific methodology for each of the event. The approach used for flood detection depends on the type of flood experienced while the drought analysis does not have such limitation. The analysis for such hydrological events should be done with a lot of care, which is due to the different properties of basins and the different type of flood and drought experienced by each

basin. Floods are short lived and they affect smaller area, thus first of all we should know the spatial extent of flood and the time period for which it affected the area. Life of flood and its spatial extent if found to be large suggests that it has high probability of being seen by GRACE (Example, for 2010 Pakistan floods and 2009 Amazon floods whole basin was analysed, see figures 4.3, and 4.41) while the smaller spatial extent and smaller life of flood makes it difficult to be seen by GRACE so, selecting only the area under flood instead of whole basin would help (example, Parana river basin analysis did not showed Sao Paulo 2004 flood, see figures 4.5 and 4.8). While droughts have large spatial extent and their life is also more than floods thus their analysis should be done at basin scale time-series and residual generation. The droughts are not visible when we have a basin under drought for long period of time (example, Nile river basin drought was not visible, see figure 4.51).

7.1.2 Outlook and recommendations

The analysis methods used, such as time-series analysis and residual analysis play a vital role, since time-series is for a short period and it contains trends (systematic signal) also thus it is difficult to visualise the outliers. The trend in New Orleans time-series affected visualisation of flooding events (see figure 4.20). The residuals remove trend and thus the systematic behaviour of signal is not a problem, so we were able to visualise the outliers in residual plots. Residuals also have one problem, the mean for integer number of years with respect to which we observe these outliers is itself calculated from just 6 years. While doing analysis with statistical tools the number years data used to get mean is not sufficient. The drought events having a life of more than 6 years, would project a mean which would show the dry conditions as normal behaviour of basin thus the outliers denoting dry conditions would not appear in such case. So, we require more data from GRACE (The next GRACE mission would do that) in order to get better residuals and better mean as representative of the basin or area under investigation. The next step would be to get to know how efficient is GRACE in showing the mass changes by these hydrological events. The validation from in-situ data, and calculation of the mass change anomaly from GRACE is what we can look forward to.

7.2 Seismology

7.2.1 Conclusions

Seismic activities such as earthquakes and volcanic activity leading mass redistribution at large spatial scale produce gravity changes can be observed by GRACE. We opted for geoid height variation over time for analysis of such events since the geoid is gradient of gravity and thus, visually it is more smoother and provides better visualisation. Earthquake activities can be observed with a magnitude more than 8.36 ideally but GRACE errors raises this limit. We were able to observe only 2 earthquakes out of 5 earthquakes which occurred in this time-period of GRACE with magnitude more than 8.36. The methodology used involves interacting tectonic plates and the epicentre. It provides a hint that tectonic plates shows a different relative geoid height anomaly with respect to each other before and after earthquake. In this study we tried to see the relative changes in geoid height anomaly of plates which was helpful in describing the type of earthquake, as the two plates were in phase for Sumatra-Andaman earthquake which was a strike-slip earthquake while for Chile earthquake the two plates were out of phase and it was thrust fault. We can monitor tectonic activities also by GRACE. We need to pay attention to ΔC_{20}, since they are affected most by any earthquake and GRACE has poor ΔC_{20} thus we should get the most accurate ΔC_{20} and replace GRACE ΔC_{20}. We replaced GRACE C_{20} by C_{20} obtained from SLR. Volcanoes pushing earth surface produce a considerable change in earth surface height leading to huge mass redistribution but the spatial extent of these volcanic area is a huge limitation in their observations. The two volcanoes observed in this master thesis are Caldera Yellowstone super-volcano and Bolivia super-volcano. The Caldera Yellowstone super-volcano showed a trend in the geoid height but the reason could be local hydrology or it might be due to rising volcano. Since there has not been any reports of increase in hydrological mass and neither any hydrological events, but there were reports declaring that the volcano has been observed to rise at a rate of 7 cm per year. So the signal is most probably due to the rising surface.

7.2.2 Outlook and recomendations

Earthquakes with intensity 8.36 and more are rare and also due to GRACE dependence on type of fault limits the number of earthquakes that can be seen. In this work the relative plate geoid height showed a behaviour which was in agreement to the type of fault occurred,

thus we can move steps towards tectonic activity monitoring by GRACE. The next GRACE mission might provide a better range rate amplitude and thus we may be able to observe even smaller magnitude earthquakes. For volcanic study further work would be to validate the findings, by using the height changes observed by GRACE to calculate mass changes and then to compare with the mass changes suggested by in-situ data for Caldera Yellowstone Volcano. The Bolivia super-volcano did not showed any sign of positive trend, rather it showed a negative trend so hydrological in-situ data, and accurate GPS height observation would clarify the reason behind negative trend.

7.3 Glaciology

7.3.1 Conclusions and recomendation

Glaciers showed a negative trend and they are in good agreement with major work that has been done so far. Due to GRACE poor spatial resolution we can not comment on the accuracy of small glaciers, such as Gangotri and Siachin glaciers observed in this thesis work. The Greenland Ice-cap was investigated earlier also by J. L. Chen [2006] and Oliver Baur [2011], and our trend analysis also showed results in agreement to accelerated melting. The Asian glaciers, Gangotri and Siachin need validation and further analysis by better spatial resolution data from GRACE. We got the trend slope for Gangotri more than Greenland while Siachin equalling the Greenland trend slope, and Walter W. Immerzeel [2010] commented that the Asian glaciers are retreating at faster speed than Greenland.

This thesis work was done with a aim to provide the initiation and the necessary understanding to analyse hydrological events such as floods and droughts, seismic activities such as earthquakes and volcanic activity. The next step would be to go for quantitative analysis with ancillary ground data to comment on how sensitive and accurate GRACE is. Definitely GRACE can observe any events posing a local gravity change due to mass redistribution over a large spatial extent but how much can we rely on GRACE. Glacier melting has already been investigated by many people and they came up with conclusion that GRACE is a potential mission to observe melting glaciers at a good temporal rate and with good accuracy.

We hope that next GRACE mission would provide data at better spatial resolution and with better accuracy, and it would help us analyse and study the phenomenon in a better manner.

Bibliography

R. Schmidt. Hydrological signals observed by the grace satellites. *Surv Geophys*, March 2008. doi: 10.1007/s10712-008-9033-3.

Michael Schmidt Florian Seitz. Signals of extreme weather conditions in central europe in grace 4-d hydrological mass variation. *Earth and Planetary Science Letters*, 268:165–170, January 2008. doi: 10.1016/j.espl.2008.01.001.

Mery Molenaar John Wahr. Time variability of the earth's gravity field: hydrological and oceanic effects and their possible detection using grace. *Geophysical Research letters*, (98JB02844), 1998.

S. Bettadpur B. D. Tapley. The gravity recovery and climate experiment: mission overview and early results. *American Geophysical Union*, 2004.

Sean Swenson John Wahr. Accuracy of grace mass estimates. *Ge*, 33, March 2006. doi: 10.1029/2005GL025305.

Katrin Bentel. Empirical orthogonal function analysis of grace gravity data. Master's thesis, Geodesy and Geoinformatics, University of Stuttgart, june 2009.

Sean Swenson John Wahr. Time-variable gravity from grace: First results. *Geophysical Research letters*, 31, May 2004. doi: 10.1029/2004GL019779.

Nico Sneeuw Oliver Baur. Assessing greenland ice mass loss by means of point-mass modeling: a viable methodology. *Journal of geodesy*, 2011. doi: 10.1007/s00190-011-0463-1.

Th.; Gntner A.; Mandea M.; Rothacher M.; Schne Flechtner, F.M.; Gruber. *System Earth Via Geodetic-Geophysical Space Techniques*. Advanced technologies in earth sciences. Springer, 2010.

Christopher Jekeli. Alternative methods to smooth the earth's gravity field. Technical report, Geodetic and geoinformation sciences, The Ohio State University, 1981.

M. J. Tourian J. Riegger. Analysis of grace uncertainties by hydrological and hydro-meteorological observations. 2010.

Isabella Velicogna Mathew Rodell. Satellite-based estimates of groundwater depletion in india. *Nature*, August 2009. doi: 10.1038/nature08238.

Jianli Chen Mathew Rodell. Estimating groundwater storage changes in the mississippi river basin (usa) using grace. *Hydrology Journal*, 15:159 – 166, September 2006. doi: 10.1007/s10040-006-0103-7.

Ludovicus P. H. Van Beek Walter W. Immerzeel. Climate change will affect the asian water towers. *sciencemag*, 328:1382–1385, 2010.

Sonia I. Seneviratne Ole B. Andersen. Grace-derived terrestrial water storage depletion associated with the european heat wave. *Geophysical Research letters*, 32, September 2005. doi: 10.1029/2005GL023574.

Stephane Calmant Flavio Guilherme Vaz de Almeida. Time-variations of equivalent water heights from grace mission and in-situ river stages in the amazon basin. *Acta Amazonica*, 42:125–134, 2012.

Paul A. Dirmeyer. Floods and droughts in a changing climate now and the future. Earthzine monthly news letter, 2011. URL `http://www.earthzine.org/2011/04/29/floods-and-droughts-in-a-changing-climate-%E2%80%93-now-and-the-future/`.

C. R. Wilson J. L. Chen and B. D. Tapley. The 2009 exceptional amazon flood and interannual terrestrial water storage change observed by grace. *WATER RESOURCES RESEARCH*, 46: W12526, December 2010. doi: 10.1029/2010WR009383.

Blake Schmidt and Gabrielle Coppola. Subway strike paralyzes sao paulo, triggers rush-hour protests, may 2012. URL `http://www.bloomberg.com/news/2012-05-23/subway-strike-paralyzes-sao-paulo-triggers-rush-hour-protests.html`.

2004 flood archive, 2005. URL `http://www.dartmouth.edu/~floods/Archives/2004sum.htm`.

2005 flood archive, 2006. URL `http://www.dartmouth.edu/~floods/Archives/2005sum.htm`.

2007 global register of major flood events, 2008a. URL `http://www.dartmouth.edu/~floods/Archives/2007sum.htm`.

More floods threaten south china, June 2008b. URL `http://news.bbc.co.uk/2/hi/asia-pacific/7459628.stm`.

Pakistan floods 2010: Latest facts, news, photos & maps, 2010. URL `http://mceer.buffalo.edu/infoservice/disasters/pakistan-floods-2010.asp`.

Larry West. Environmental issues. URL `http://environment.about.com/od/environmentalevents/a/whatisdrought.htm`.

Rhett A. Butler. Amazon drought continues, worst on record, December 2005. URL `http://news.mongabay.com/2005/1211-amazon.html`.

Paul Tregoning marc J. Leblanc. Basin-scale, integrated observation of the early 21st century multiyear drought in southeast australia. *Water resource research*, 45:W04408, 2009. doi: 10.1029/2008WR007333.

HIROO KANAMORI and DON L. ANDERSON. Theoretical basis of some empirical relations in seismology. *Bulletin of the Seismological Society of America*, 65:1073–1096, October 1975.

Richard S. Gross B. Fong Chao. Changes in the earth's rotation and low-degree gravitational field induced by earthquakes. *Geophysical Research letters*, 91:569–596, 1987.

David C. McAdoo Carl A. Wagner. Time variations in the earth's gravity field detectable with geopotential research mission intersatellite tracking. *JOURNAL OF GEOPHYSICAL RESEARCH*, 91, B8, March 1986. doi: 10.1029/JB091iB08p08373.

C. K. Shum Shin-Chan Han. Crustal dilatation observed by grace after the 2004 sumatra-andaman earthquake. *Science*, 313:658–662, 2006.

Jeanne Sauber Shin-Chan Han. Regional gravity decrease after the 2010 maule(chile) earthquake indicates large-scale mass redistribution. *Geophysical Research letters*, 37, 2010. doi: 10.1029/2010GL045449.

C. R. Wilson J. L. Chen. Satellite gravity measurements confirm accelerated melting of greenland ice sheet. *Science*, 313:1958–1960, 2006. doi: 10.1126/science.1129007.

Anthony A. Arendt Scott b. Luthcke. Recent glacier mass changes in the gulf of alaska region from grace mascon solutions. *Journal of Glaciology*, 54:767–777, 2008.

x

Appendix A

Data set levels

The GRACE products are developed, processed and archived in a shared Science Data System (SDS) between the Jet Propulsion Laboratory (JPL), the University of Texas Center for Space Research (UTCSR) and the GeoForschungsZentrum Potsdam (GFZ).

The level-0 to level-2 products are defined as follows:

- Level-0:

  The level-0 data are the result of the data reception, collection and decommutation by the Raw Data Center (RDC) of the Mission Operation System (MOS) located in Neustrelitz, Germany. The MOS receives twice per day using its Weilheim and Neustrelitz tracking antennae the science instrument and housekeeping data from each GRACE satellite which will be stored in two appropriate files in the level-0 rolling archive at DFD/Neustrelitz. The SDS retrieves these files and extracts and reformats the corresponding instrument and ancillary housekeeping data like GPS navigation solutions, space segment temperatures or thruster firing events. Level-0 products are available 24 hours after data reception.

- Level-1:

  The level-1 data are the preprocessed, time-tagged and normal-pointed instrument data. These are the K-band ranging, accelerometer, star camera and GPS data of both satellites. Additionally the preliminary orbits of both GRACE satellites will be generated. Level-1 data processing software is developed by JPL with support from GFZ (e.g. accelerometer data preprocessing). Processing of level-1 products is done primarily at JPL. An identical processing system (hardware/software) is installed at GFZ to serve as a backup system in case of hardware or network problems. This double implementation is necessary to guarantee the envisaged level-1 product delay of 5 days. All level-1 products are archived at JPL's Physical Oceanography Distributed Active Data Center (PODAAC) and at GFZ's Integrated System Data Center (ISDC) . Both archives are harmonized on a sub-daily timeframe.

- Level-2:

  Level-2 data include the short term (30 days) and mean gravity field derived from calibrated and validated GRACE level-1 data products. This level also includes ancillary data sets (temperature and pressure fields, ocean bottom pressure, and hydrological data) which are necessary to eliminate time variabilities in gravity field solutions. Additionally the precise orbits of both GRACE satellites are generated. All level-2 products

are archived at JPL's PODAAC and at GFZs ISDC and are available 60 days after data taking. The level-2 processing software were developed independently by all three processing centres using already existing but completely independent software packages which were upgraded for GRACE specific tasks. Common data file interfaces guarantees a strong product validation. Routine processing is done at UTCSR and GFZ, while JPL only generate level-2 products at times for verification purposes.

Appendix B

Data format

The data consists of number of months $\times$ 10 matrix of cell type structure. First column describes model in our case it is EIGEN. Second describes type of model, which can be amongst GSM, GSD, GAD, GAC, GAA, and GAB. Where in the three letters signify the nature of data.

- First character G stands for geopotential coefficients.
- Second character if is:
    1. S, means Estimates from only GRACE data.
    2. C, means combination estimates from GRACE and terrestrial gravity information.
    3. E, means any background model specified as a time-series.
- And lastly third character if is:
    1. M: means estimate of the static field.
    2. U, means geopotential estimates relative to the background gravity model.
    3. T, means total background gravity model except for background static model.
    4. A, means non-tidal atmosphere.
    5. B, means non-tidal oceans.
    6. C, means combination of non-tidal atmosphere and ocean, and
    7. if is D, it means bottom pressure over oceans, zero over land.

I used GSM thus the coefficients are geopotential coefficients of static field estimated only from GRACE data.

Third column tells the release level, in our case it was level 04. The fourth column tells year, fifth tells the month. The sixth column contains start day, end day, and number of days considered for observation. Next is seventh column which tells the version, it contains numeral either 0 or 2, 0 tells that the solution is not regularized and 2 tell that the solution is regularized. Eighth column tells the maximum degree and order of the coefficients; it is 120 for the data I used. Ninth column contains Spherical harmonic coefficients. And the tenth column has error estimates. The organization of coefficients is in C-S format, the diagonal from first row first column element to last row last column in the spherical harmonic coefficients matrix divides it into C_{nm} and S_{nm}. The coefficients in south-west triangular matrix are C_{nm} and in north-east triangular matrix are S_{nm}.